AD-A015 065

RESEARCH IN SEISMOLOGY: EARTHQUAKE MAGNITUDES

Otto W. Nuttli, et al

Saint Louis University

Prepared for:

Air Force Cambridge Research Laboratories
Advanced Research Projects Agency

18 July 1975

AFCRL-TR-75-0433

RESEARCH IN SEISMOLOGY: EARTHQUAKE MAGNITUDES

Otto W. Nuttli
So Gu Kim
Huei-Yuin Wen

Department of Earth and Atmospheric Sciences
Saint Louis University
St. Louis, Missouri 63103

18 July 1975

Scientific Report No. 3

Approved for public release; distribution unlimited.

Sponsored by
Defense Advanced Research Projects Agency
ARPA Order No. 1795, Amendment #4
Monitored by
AIR FORCE CAMBRIDGE RESEARCH LABORATORIES
AIR FORCE SYSTEMS COMMAND
UNITED STATES AIR FORCE
HANSCOM AFB, MASSACHUSETTS 01731

ARPA Order No. 1795
Program Code No. 3F10
Contractor: Saint Louis University
Effective Date of Contract: 1 July 1973

Contract No. F19628-73-C-0269
Principal Investigator & Phone No.
Dr. Otto W. Nuttli/314 535-3300
Ext. 547B
AFCRL Project Scientist & Phone No.
Stanley M. Needleman
Contract Expiration Date:
31 December 1975

Qualified requestors may obtain additional copies from the Defense Documentation Center. All others should apply to the National Technical Information Service.

Unclassified

SECURITY CLASSIFICATION OF THIS PAGE (When Data Entered)

REPORT DOCUMENTATION PAGE		READ INSTRUCTIONS BEFORE COMPLETING FORM
1. REPORT NUMBER AFCRL-TR-75-0433	2. GOVT ACCESSION NO.	3. RECIPIENT'S CATALOG NUMBER
4. TITLE (and Subtitle) RESEARCH IN SEISMOLOGY: EARTHQUAKE MAGNITUDES		5. TYPE OF REPORT & PERIOD COVERED Scientific - Interim
		6. PERFORMING ORG. REPORT NUMBER Scientific Report No. 3
7. AUTHOR(s) Otto W. Nuttli, So Gu Kim and Huei-Yuin Wen		8. CONTRACT OR GRANT NUMBER(s) F19628-73-C-0269
9. PERFORMING ORGANIZATION NAME AND ADDRESS Dept. of Earth and Atmospheric Sciences Saint Louis University St. Louis, MO 63103		10. PROGRAM ELEMENT, PROJECT, TASK AREA & WORK UNIT NUMBERS PE 62701E- Project 1795 T,WU & SE n/a
11. CONTROLLING OFFICE NAME AND ADDRESS Air Force Cambridge Research Laboratories Hanscom AFB, MA 01731 Contract Monitor: Stanley M. Needleman/LWW		12. REPORT DATE 18 July 1975
		13. NUMBER OF PAGES 51
14. MONITORING AGENCY NAME & ADDRESS(if different from Controlling Office)		15. SECURITY CLASS. (of this report) Unclassified
		15a. DECLASSIFICATION/DOWNGRADING SCHEDULE

16. DISTRIBUTION STATEMENT (of this Report)

Approved for public release; distribution unlimited.

17. DISTRIBUTION STATEMENT (of the abstract entered in Block 20, if different from Report)

18. SUPPLEMENTARY NOTES

This research was sponsored by the Defense Advanced Research Projects Agency under ARPA Order No. 1795, Amendment #4.

19. KEY WORDS (Continue on reverse side if necessary and identify by block number)

Nuclear explosions
Earthquakes
Magnitudes
Seismic discrimination
Eurasia
Aftershocks

20. ABSTRACT (Continue on reverse side if necessary and identify by block number)

This report presents data on the body (m_b) and surface-wave (M_S) magnitudes of 159 Eurasian earthquakes and underground explosions that occurred during the interval 1 January through 30 June 1972. The number of earthquakes found to be anomalous by the m_b:M_S criterion alone can be reduced if in addition an $M_{S,RZ}$:$M_{S,L}$ criterion is employed. It was also found that for some aftershock sequences the later events in the sequence tend to have a more explosion-like m_b:M_S value.

DD FORM 1 JAN 73 1473 EDITION OF 1 NOV 65 IS OBSOLETE

Unclassified

SECURITY CLASSIFICATION OF THIS PAGE (When Data Entered)

1. INTRODUCTION

This report presents the findings of and summarizes the research activity for the 12-month interval 1 July 1974 through 30 June 1975. During that time principal effort was devoted to gathering and analyzing body- (m_b) and surface-wave (M_S) magnitudes for small and intermediate magnitude events in and near Eurasia, in order to seek out shallow depth earthquakes which appear anomalous according to the m_b:M_S criterion. In the next phase of the study we shall concentrate on seeking explanations as to why certain earthquakes are anomalous according to that criterion, and, if possible, in developing a methodology to predict where such anomalous earthquakes will occur.

The procedures used in determining m_b and M_S values are standard ones. However, inasmuch as there are slight differences among investigators in applying the standard procedures, a brief description of our methods will be given.

The m_b values are determined by use of the Gutenberg-Richter (1956) equation

$$m_b = \log (A/T) + Q(h,\Delta) \qquad (1)$$

where (A/T) is taken as one-half the maximum peak-to-peak motion (in microns/second) in the first three cycles of the vertical component of the P-wave ground motion in the period range of 0.7 to 1.3 seconds. As a further restriction we determine m_b values only from stations at teleseismic distances, i.e. greater than or equal to 25°, because at lesser distances the lateral variations in upper mantle structure make the function Q dependent on geographical region.

The M_S values are determined by use of the IASPEI formula (Båth, 1969)

$$M_S = 3.30 + 1.66 \log \Delta + \log (A/T) \quad \text{for } 25^\circ \leq \Delta \leq 140^\circ \qquad (2)$$

and the Nuttli-Kim (1975) formula

$$M_S = 4.16 + 1.07 \log \Delta + \log (A/T) \quad \text{for } 10^\circ \leq \Delta \leq 25^\circ \qquad (3)$$

where (A/T) is taken as one-half the maximum peak-to-peak motion (in microns/second) of the vertical component of the Rayleigh-wave ground motion in the period range of 17 to 23 seconds. The quantity Δ is the epicentral distance, measured in degrees.

The m_b value is a measure of the ground-motion spectrum at a period of 1 second and the M_S value a measure of the ground-motion spectrum at a period of 20 seconds. From this it follows that surface-wave magnitude formulas that pretend to measure M_S by making use of shorter period surface waves (e.g. the formulas of Karnik et al, 1962; Evernden et al, 1971; Basham, 1971; Nuttli, 1973) cannot be valid over the entire range of magnitudes because the shorter period motion does not scale the same as the 20-second period motion over the entire range of magnitudes (see, e.g., Aki, 1967,1972; Duda and Nuttli, 1974).

2. THE DATA

Table 1 gives the hypocentral coordinates and geographical location of the 155 earthquakes and 4 underground explosions that are the subject of this report. All occurred in or near Eurasia during the interval 1 January 1972 through 30 June 1972, and all were found to be of shallow depth by the NEIC (National Earthquake Information Center). Independent depth estimates made by the ISC (International Seismological Centre) are also given in Table 1.

Table 2 gives the m_b and M_S values of the events studied. Standard deviations of the mean of the m_b and M_S values determined by us are also included. The symbol $M_{S,RZ}$ refers to surface-wave magnitude determined from the vertical component of the Rayleigh-wave motion, and the symbol $M_{S,L}$ to surface-wave magnitude determined from the Love-wave motion. Because for underground explosions $M_{S,L}$ is one or more units less than $M_{S,RZ}$, whereas for earthquakes they are of about the same value, the $M_{S,L}:M_{S,RZ}$ value is another useful discriminant between earthquakes and explosions. The $M_{S,L}$ values given in this report were determined from the data of horizontal-component instruments that were transverse (within 20°) to the ray path at the seismograph station.

3. INTERPRETATION OF THE DATA

3.1. m_b estimates

Table 2 contains 3 independent estimates of the m_b value of each event. The NEIC and ISC estimates are based on amplitude data sent by individual seismograph stations to a central agency. Our estimates, on the other hand, are based on amplitudes read by us from film copies of WWSSN seismograms for a

selected number of stations. In general the number of stations employed by us to estimate m_b is less than that used by NEIC and ISC, because we used only a selected group of stations and because we do not use amplitude data from stations at epicentral distances of less than 25°.

To compare the 3 sets of m_b estimates with each other, we first found the difference between the NEIC values (arbitrarily taken as standard) and the ISC and our values. Fig. 1 shows histograms for the absolute value of these magnitude differences, broken down into 3 magnitude ranges. For the ranges $4.1 \leq m_b \leq 4.5$ and $4.6 \leq m_b \leq 5.0$ approximately 50% of the deviations are no greater than 0.1 unit, and for $5.1 \leq m_b \leq 5.5$ approximately 60% of the deviations are no greater than 0.1 unit. Therefore, on the average, differences in the 3 sets of m_b values are not large enough to affect the values used in the m_b:M_S criterion. There are exceptions, however. As can be seen in Fig. 1, the absolute deviations were as large as 1.2 units. In particular, for earthquakes in Italy, Yugoslavia and the Greenland Sea the NEIC values in some cases were 0.9 or more units larger than the ISC or our values. We have found that in general the NEIC tends to overestimate m_b values in Central Europe.

3.2. Standard deviation of m_b and M_S estimates

Fig. 2 presents histograms showing the standard deviation of our m_b and M_S values. The figure shows that the majority of the values of the standard deviation of m_b fall in the range of 0.3 to 0.4 units; the corresponding value for M_S is 0.3 units.

3.3. Plots of m_b:M_S data

Figs. 3, 4 and 5 present the m_b:M_S values. For Fig. 3 the m_b values are those of the NEIC, for Fig. 4 those of the ISC and for Fig. 5 the m_b values are ours. In all cases the M_S values are ours, inasmuch as the ISC gave no M_S values and the NEIC gave them for only a few earthquakes.

The solid-line curve in Figs. 3, 4 and 5 is the m_b:M_S curve for Nevada Test Site explosions as given by Evernden et al (1971) when they used the amplitude of 20-second period Rayleigh waves to determine M_S. This curve was shown to satisfy the data for Soviet underground explosions which took place from 1 August 1971 through 31 December 1971 (Nuttli and Kim, 1975).

The dotted line in Figs. 3, 4 and 5 is the 5% earthquake line of Marshall and Basham (1972). That is, Marshall and Basham found that 95% of the earthquakes they studied had

m_b:M_S values that fell to the right of the dotted line.

The dashed line in Figs. 3, 4 and 5 is displaced 0.46 units to the right and below the solid-line curve, as measured perpendicular to the solid-line curve. The number 0.46 was arrived at by taking the vector resultant of the average of the m_b and M_S standard deviations, whose values were given in section 3.2.

Using the NEIC m_b values and our M_S values, the following earthquakes fall to the left of both Marshall and Basham's (1972) and our curve: 1, 16, 22, 31, 54, 62, 78, 79, 86, 91, 101, 106, 111, 116, 120, 123, 131, 133, 134, 135, 137, 146, 148, 156, 157, 158. In addition, events 45, 102, 117, 130, 136 fall to the left of Marshall and Basham's curve and events 21, 36, 43, 76, 77, 107, 110, 145 fall to the left of our curve. Using the ISC m_b values and our M_S values, events 11, 31, 54, 79, 103, 111, 123, 135, 146 fall to the left of both curves, events 1, 45, 91, 130 to the left of the Marshall and Basham curve and events 21, 43, 106, 129, 145 to the left of our curve. Using our m_b and M_S values, events 37, 103, 145, 146 fall to the left of both curves, event 45 to the left of the Marshall and Basham curve and events 43, 55, 73, 135, 148 to the left of our curve.

From the above, as well as from Figs. 3, 4 and 5, we can conclude that the NEIC m_b values tend to be larger than the ISC or our m_b values and thus give rise to the largest number of apparently anomalous earthquakes. This is not too surprising, for the NEIC is the first organization to publish hypocentral and magnitude data. Thus the only stations that send amplitude data to NEIC are those with relatively strong P arrivals. The ISC and our determinations, on the other hand, are made after an approximate hypocenter is available, so that we know the time when the P wave is expected; thus we will read P-wave amplitudes at stations where the arrival is not necessarily strong.

3.4. Anomalous earthquakes

Table 3 gives the location of all the earthquakes found to be anomalous by either the Marshall and Basham (1972) or our criterion(less than one standard deviation from the explosion curve) and for any of the NEIC, ISC or our m_b values. The table shows that most, but not all, of the anomalous earthquakes occur in the interior of Eurasia. The most frequently appearing anomalous source regions in Asia are in Szechwan and Sinkiang provinces of China, Tadzhikistan, Pakistan and Tibet.

Love-wave magnitudes can be used to reduce the number of anomalous events by making use of the observation that for underground explosions $M_{S,L}$ is observed to be 1 or more units smaller than $M_{S,RZ}$, whereas for earthquakes they both have approximately the same value. Therefore, conservatively, it can be concluded that any event for which $M_{S,L}$ is greater than or equal to $M_{S,RZ} - 0.5$ must be an earthquake. By this criterion events number 1, 11, 16, 22, 31, 37, 45, 62, 101,102, 103, 106, 107, 111, 116, 117, 120, 123, 131, 133, 134, 135, 136, 146, 156, 157 can be definitely identified as earthquakes, even though their $m_b:M_{S,RZ}$ values are anomalous.

When both the $m_b:M_{S,RZ}$ and $M_{S,L}:M_{S,RZ}$ criteria are employed, the list of anomalous earthquakes is reduced to events no. 22, 36, 43, 54, 55, 73, 76, 77, 78, 79, 86, 91, 110, 129, 130, 137, 145, 148, 158. Of these, events 22, 36, 76, 77, 78, 86, 110, 137, 158 are anomalous only if the NEIC m_b value is used.

4. AFTERSHOCK SEQUENCES

Previously it was noted that the majority of anomalous earthquakes were found to occur within Eurasia, rather than on its oceanic boundaries. It can be seen from Figs. 3, 4 and 5 than in general the earthquakes in the interior tend to lie in the more explosion-like part of the $m_b:M_S$ plot. Fig. 6 is an example of an aftershock sequence in Szechwan province of China which shows earthquakes that are anomalous or near-anomalous by the $m_b:M_S$ criterion.

In Fig. 6 the earthquakes of 16 August (1) and 03 September fall on the explosion side of the Marshall-Basham and our curve. Although the remaining earthquakes are on the earthquake side of the curves, they lie relatively close to the curves.

It is of some interest to determine if the position of the plotted points in Fig. 6 is controlled by the radiation of earthquake energy or rather by errors in reading the wave amplitudes, because of contamination by noise. In an attempt to investigate this problem, we have looked at both the time history and the spectra of earthquakes no. 1, 2 and 3 of 16 August, to determine if no. 1 belongs on the explosion side of the curves and nos. 2 and 3 on the earthquake side.

Figs. 7 and 8 show the vertical-component Rayleigh-wave spectra for stations COL (College, Alaska) and AQU (Aquila, Italy), respectively. The epicentral distance to COL is 71.6° and to AQU is 71.4°, so that they are almost at the same distance from the epicenter. Their ray paths are entirely different, however; the back azimuth to COL is 299° and to AQU is 68°. An inspection of Figs. 7 and 8 will show

that the minimum (or hole) in the spectra occurs at the same period, approximately 40 seconds, for all 3 earthquakes, indicating that each of the earthquakes had the same focal depth. Also, we can see that the spectral level of earthquake 2 is the largest, followed by 1 and then 3. This agrees qualitatively with the M_S values of the three earthquakes.

Figs. 9 and 10 show the vertical-component Rayleigh-wave seismograms for COL and AQU, respectively. From these figures also it can be seen that the largest Rayleigh waves correspond to earthquake 2, and the smallest to earthquake 3.

Figs. 11 and 12 contain the spectra of the vertical component of the P-wave motion, as obtained from the long period seismograms. Because of the dynamic response of the seismograph system, the spectra obtained from these instruments are only valid down to a period of about 2 seconds. Because a time window of 20 seconds was used, these spectra are only valid up to a period of about 10 seconds. The spectra are fitted by two straight-line segments between 2 and 10 seconds, a horizontal line for the longer period part and one which has a slope of -2 for the shorter period part. The period at which the two lines intersect is called the corner period.

From Figs. 11 and 12 we can see that the amplitude level of the T^{-2} curve at 1-second period is greatest for earthquake no. 1, next for no. 3 and least for no. 2. From the m_b values shown in Fig. 6 one would expect earthquake no. 1 to have the largest spectral amplitude at a period of 1 second, and no. 2 to have a slightly larger value than no. 3.

Figs. 13 and 14 show the vertical-component short-period P-wave seismograms for COL and AQU, respectively. In Fig. 12 the largest P wave occurs for earthquake no. 1, then 2 and finally 3, as expected from the m_b values of the 3 earthquakes. However, the P-wave amplitudes at AQU are almost the same for all 3 earthquakes.

Referring back to Figs. 11 and 12, we can see that the corner period at COL and AQU for earthquake no. 2 is about 6 seconds, whereas for no. 1 and 3 it is about 3.5 seconds. The longer corner period for no. 2 would indicate a lesser stress drop for it and consequently a higher long period spectral level, or a higher M_S value, as observed.

In summary, the 3 earthquakes had about the same focal depth and the same epicenter, so the differences in their

characteristics cannot be related to their location in the source region. In general, the differences in their $m_b:M_S$ values are reflected both in the time histories of the short and long period, vertical-component motions, and also in the spectra of the long period P and Rayleigh waves. It appears that earthquakes in an aftershock sequence which have about the same magnitude can have spectra with different corner periods, probably a result of difference in the stress drops. This can lead to different $m_b:M_S$ values for earthquakes of about the same "size."

Figure 15 shows $m_b:M_S$ values for the main shock and aftershocks of a sequence in south Sinkiang province, China. The main shock, earthquake no. 1 of 15 January, falls slightly on the earthquake side of the curves. Some of the later aftershocks have $m_b:M_S$ values lying even closer to the curves. In general there is a tendency for the later aftershocks to move closer to the curves, or to cross over to the explosion side of them. The same phenomenon can be seen in Fig. 16, which is for an aftershock sequence that occurred off the east coast of Honshu Island, Japan. For that sequence, however, none of the aftershocks had $m_b:M_S$ values that put them on the explosion side of the curve.

A phenomenon similar to that shown by Figs. 6, 15 and 16, i.e. a tendency for aftershocks to migrate to the more explosion-like part of the $m_b:M_S$ plot, appears in data presented by Landers (1972) for an aftershock series in Tibet in 1968, and in data presented by Tsai and Patton (1973) for the San Fernando, California sequence of 1971. The significance of their observations with regard to nuclear explosion discrimination problems did not appear to be recognized by these authors, or at least not given much emphasis.

The use of aftershocks to conceal an explosion has been suggested as one way to evade detection of the explosion. Our findings that the later earthquakes in an aftershock sequence can have near explosion-like $m_b:M_S$ values, at least for certain earthquake sequences, makes this evasion technique look even more promising.

It should be emphasized that we are not stating that all aftershock sequences show a progression from more earthquake-like to more explosion-like events. But some do behave this way, as shown in the examples given above.

5. CONCLUSIONS

From a study of 155 shallow depth earthquakes and 4 underground explosions in and near Eurasia we found that approximately 25% of the earthquakes are anomalous by the m_b:M_S criterion if the NEIC m_b values are used. This number is reduced to 12% if the ISC m_b values are used and to 6% if our m_b values are used. In general the NEIC has larger m_b values, particularly for events in Central Europe.

By using both the m_b:M_S and $M_{S,RZ}$:$M_{S,L}$ criteria the percentage of anomalous earthquakes is reduced to 12% if the NEIC m_b values are used, 5% if the ISC m_b values are used, and 3% if our m_b values are used. These percentages might be further reduced if the Love-wave motion were obtained by digitizing the horizontal-component seismograms at each station and by rotating coordinates so as to have one horizontal component perpendicular to the great-circle path and the other along it. We intend to do this in future studies of some of the anomalous earthquakes. For the present, however, we determined $M_{S,L}$ only from stations for which the great-circle path was within 20° of the N-S or E-W directions.

Using both the m_b:M_S and $M_{S,RZ}$:$M_{S,L}$ criteria and either the m_b values of the ISC or those found by us, the anomalous Eurasian earthquakes for 1 January 1972 through 30 June 1972 are: no. 21 (Central Italy), 43 (Tibet), 54 (Yugoslavia), 55 (S. Sinkiang), 91 (N. Sinkiang), 129 (Greece-Bulgaria), 130 (E. Honshu) and 145 (Caspian Sea). This is about 6% of the total number of events considered.

A study of the m_b:M_S values in aftershock sequences indicated that for some sequences there is a progression in time from a more earthquake-like main shock to more explosion-like aftershocks. This is not necessarily true of all aftershock sequences, but for those in which it does occur it would tend to aid in evading detection of an explosion set off in the later part of such a sequence.

5. REFERENCES

Aki, K. (1967). Scaling law of seismic spectrum, Journal of Geophysical Research, 72, 1217-1231.

Aki, K. (1972). Scaling law of earthquake source time-function, Geophysical Journal of the Royal Astronomical Society, 31, 3-25.

Basham, P. W. (1971). A new magnitude formula for short period continental Rayleigh waves, Geophysical Journal of the Royal Astronomical Society, 23, 255-260.

Båth, M. (1969). Handbook of Magnitude Determinations, Seismological Institute, Uppsala, Sweden.

Duda, S. J. and O. W. Nuttli (1974). Earthquake magnitude scales, Geophysical Surveys, 1, 429-458.

Evernden, J. F., W. J. Best, P. W. Pomeroy, T. V. McEvilly, J. M. Savino and L. R. Sykes (1971). Discrimination between small-magnitude earthquakes and explosions, Journal of Geophysical Research, 76, 8042-8055.

Karnik, V., N. V. Kondorskaya, Y. V. Riznichenko, E. F. Savarensky, S. L. Soloviev, N. V. Shebalin, J. Vanek and A. Zatopek (1962). Standardization of the earthquake magnitude scale, Studia Geophysica et Geodetica, 6, 41-47.

Landers, T. (1972). Some interesting central Asian events on the $M_S:m_b$ diagram, Geophysical Journal of the Royal Astronomical Society, 31, 329-339.

Marshall, P. D. and P. W. Basham (1972). Discrimination between earthquakes and underground explosions employing an improved M_S scale, Geophysical Journal of the Royal Astronomical Society, 28, 431-458.

Nuttli, O. W. (1973). Seismic wave attenuation and magnitude relations for eastern North America, Journal of Geophysical Research, 78, 876-885.

Nuttli, O. W. and S. G. Kim (1975). Surface-wave magnitudes of Eurasian earthquakes and explosions, Bulletin of the Seismological Society of America, 65, 693-709.

Tsai, Y. B. and H. J. Patton (1973). Dislocation Motion and Far-Field Source Spectra of Four California Earthquakes. Semi-Annual Technical Report No. 2, Contract AFOSR F44620-72-C-0073.

TABLE 1. HYPOCENTRAL COORDINATES OF EVENTS STUDIED

Event No.[a]	Date	Origin Time[b]	Lat. (^{o}N)[b,c]	Long. (^{o}E)[b]	Depth (km) NEIC	Depth (km) ISC	Location
1	02-01-72	10-27-34.9	41.8	84.5	33	11	S. Sinkiang
2	03-01-72	06-36-37.9	51.6	159.4	33	32	Kamchatka
3	03-01-72	17-06-22.3	51.1	178.9	46	40	Rat Isl.
4	03-01-72	17-26-24.8	51.2	178.8	46	46	Rat Isl.
5	03-01-72	17-31-29.4	51.1	178.9	46	42	Rat Isl.
6	03-01-72	20-01-22.5	51.1	179.0	43	41	Rat Isl.
7	05-01-72	01-05-08.7	32.9	49.2	45	59	W. Iran
8	05-01-72	02-16-10.1	43.8	147.2	33	41	Kurile Isl.
9	05-01-72	04-57-40.8	47.8	16.2	11	11	Austria
10	06-01-72	06-30-35.6	40.7	72.4	33	61	Kirgiziya
11	06-01-72	09-41-33.2	30.3	50.5	41	24	Iran
12	13-01-72	17-24-22.6	61.9	147.1	33	33	E. Siberia
13	14-01-72	22-10-03.7	32.8	46.9	33	40	Iran-Iraq
14	15-01-72	18-07-57.8	57.4	120.7	13	7	E. Russia
15	15-01-72	20-21-50.1	40.3	79.0	33	9	S. Sinkiang
16	15-01-72	23-45-59.3	40.2	78.7	33	41	S. Sinkiang
17	18-01-72	21-12-01.7	37.5	48.7	33	33	N. W. Iran
18	18-01-72	23-26-11.9	44.2	8.2	25	25	N. Italy
19	23-01-72	02-06-01.2	23.6	102.7	33	33	Yunnan
20	25-01-72	10-02-40.3	53.9	160.9	33	34	E. Kamchatka
21	25-01-72	20-24-38.9	43.8	13.4	33	0	Central Italy
22	25-01-72	23-22-17.1	43.8	13.4	33	33	Central Italy
23	26-01-72	10-50-09.2	43.9	13.3	33	21	Central Italy
24	26-01-72	18-52-23.1	42.8	145.5	48	52	Hokkaido
25	29-01-72	11-12-38.0	40.2	143.8	19	3	E. Honshu
26	02-02-72	19-13-19.8	10.2	93.8	45	44	Andaman Isl.
27	03-02-72	02-29-21.9	40.7	48.4	39	40	E. Caucasus
28	03-02-72	07-22-48.5	23.4	102.4	33	33	Yunnan
29	04-02-72	02-42-18.9	43.8	13.3	25	25	Central Italy

TABLE 1 (Cont'd)

Event No.[a]	Date	Origin Time[b]	Lat.(^{o}N)[b,c]	Long.(^{o}E)[b]	Depth (km) NEIC	ISC	Location
30	04-02-72	09-18-31.5	43.9	13.2	23	25	Central Italy
31	04-02-72	14-08-21.7	30.3	84.6	18	18	Tibet
32	04-02-72	16-33-17.7	13.2	49.4	33	45	Gulf of Aden
33	05-02-72	05-05-50.7	43.7	13.4	33	2	Central Italy
34	05-02-72	07-08-12.9	43.9	13.3	33	33	Central Italy
35	06-02-72	01-34-22.4	44.0	13.2	33	30	Central Italy
36	06-02-72	07-30-11.4	41.6	82.2	33	33	S. Sinkiang
37	09-02-72	11-22-51.7	43.2	46.0	36	58	E. Caucasus
38E	10-02-72	05-02-57.3	50.0	78.9	0	0	E. Kazakhstan
39	11-02-72	05-55-46.4	39.9	77.4	23	39	S. Sinkiang
40	11-02-72	21-36-17.0	56.1	162.9	44	12	E. Kamchatka
41	16-02-72	23-19-19.7	41.7	80.7	29	40	S. Sinkiang
42	18-02-72	18-02-34.1	43.6	147.8	36	50	Kurile Isl.
43	20-02-72	03-02-14.0	34.6	80.3	33	33	Tibet
44	21-02-72	23-02-55.5	41.0	22.3	33	0	Yugoslavia
45	22-02-72	18-43-42.0	10.4	92.5	33	4	Andaman Isl.
46	26-02-72	18-56-13.2	27.1	100.9	33	133	Yunnan Prov.
47	26-02-72	23-31-09.6	50.6	97.3	33	36	USSR-Mongolia
48	27-02-72	10-03-02.6	87.0	53.5	33	20	Franz Joseph Land
49	28-02-72	02-04-35.0	40.4	29.1	6	6	Turkey
50	29-02-72	20-54-21.2	42.0	15.4	33	0	S. Italy
51	02-03-72	09-54-28.9	20.3	120.5	33	14	Philippine Isl.
52	02-03-72	12-10-41.5	20.2	123.0	33	174	Philippine Isl.
53	02-03-72	12-48-48.5	72.4	3.3	33	33	Norwegian Sea
54	03-03-72	21-26-51.3	44.7	18.4	32	0	Yugoslavia
55	04-03-72	08-22-16.6	42.1	83.3	33	33	S. Sinkiang
56	05-03-72	06-05-29.8	14.5	56.4	33	33	Arabian Sea
57	07-03-72	06-19-50.0	22.3	122.2	33	7	Taiwan
58	08-03-72	21-49-10.6	27.6	56.7	45	67	S. Iran

TABLE 1 (Cont'd)

Event No.[a]	Date	Origin Time[b]	Lat. (^{o}N)[b,c]	Long. (^{o}E)[b]	Depth (km) NEIC	ISC	Location
59E	10-03-72	04-56-57.4	49.8	78.2	0	0	E. Kazakhstan
60	10-03-72	14-36-16.5	33.8	72.7	45	40	Pakistan
61	11-03-72	04-32-27.3	22.5	123.9	31	45	SE. of Taiwan
62	15-03-72	06-00-32.4	30.4	84.5	33	12	Tibet
63	17-03-72	07-20-07.6	27.0	127.7	38	59	Ryukyu Isl.
64	17-03-72	09-17-10.5	40.1	69.7	26	43	Tadzhikistan
65	19-03-72	13-33-15.0	24.1	121.9	39	44	Taiwan
66	21-03-72	00-57-42.5	53.0	159.7	46	64	E. Kamchatka
67	21-03-72	01-35-18.8	41.2	144.4	40	36	Hokkaido
68	22-03-72	00-51-51.6	40.3	42.1	34	2	Turkey
69	22-03-72	02-59-09.0	53.0	159.6	41	54	E. Kamchatka
70	24-03-72	08-11-52.8	42.9	87.4	33	39	N. Sinkiang
71	24-03-72	22-56-24.7	53.1	159.7	41	38	E. Kamchatka
72	25-03-72	05-58-08.2	45.4	100.8	33	79	Mongolia
73	26-03-72	06-10-33.2	25.9	93.9	33	88	E. India
74E	28-03-72	04-21-57.2	49.7	78.2	0	0	E. Kazakhstan
75	02-04-72	03-34-27.8	36.1	73.6	47	49	N. W. Kashmir
76	03-04-72	01-29-28.5	41.5	79.3	33	66	Kirgiziya-Sinkiang
77	05-04-72	13-19-47.3	42.0	84.6	33	18	N. Sinkiang
78	08-04-72	06-42-13.3	29.7	89.5	33	49	Tibet
79	09-04-72	10-43-56.3	42.0	84.6	33	46	S. Sinkiang
80	09-04-72	22-47-36.8	35.1	74.6	49	53	N.W. Kashmir
81	10-04-72	02-06-53.2	28.4	52.8	33	11	S. Iran
82	10-04-72	02-34-31.5	28.4	52.9	33	80	S. Iran
83	10-04-72	20-27-07.5	28.4	52.9	33	43	S. Iran
84	11-04-72	06-00-04.6	37.4	62.0	33	20	Turkmeniya
85	11-04-72	06-21-10.0	42.0	84.4	33	16	N. Sinkiang
86	12-04-72	18-37-40.8	28.3	53.1	33	58	S. Iran
87	16-04-72	10-10-03.6	47.7	16.1	18	18	Austria

TABLE 1 (Cont'd)

Event No.[a]	Date	Origin Time[b]	Lat. (^{o}N)[b,c]	Long. (^{o}E)[b]	Depth (km) NEIC	Depth (km) ISC	Location
88	17-04-72	02-24-49.3	34.0	72.9	45	52	Pakistan
89	17-04-72	04-04-25.8	49.3	153.0	33	219	Kurile Isl.
90	18-04-72	23-27-36.4	40.0	51.3	33	49	Caspian Sea
91	20-04-72	00-35-56.7	42.0	84.6	33	20	N. Sinkiang
92	21-04-72	21-19-29.5	35.0	81.0	33	21	Tibet
93	24-04-72	19-30-26.8	23.9	121.5	33	32	Taiwan
94	25-04-72	19-30-09.3	13.4	120.3	50	38	Manila
95	26-04-72	06-18-44.9	13.5	120.5	33	41	Philippine Isl.
96	26-04-72	09-44-23.6	13.2	120.3	50	65	Philippine Isl.
97	26-04-72	18-38-51.7	13.5	120.7	46	54	Philippine Isl.
98	28-04-72	00-52-56.8	31.3	84.9	33	32	Tibet
99	30-04-72	00-13-26.3	13.3	120.4	33	66	Philippine Isl.
100	01-05-72	20-01-15.8	23.7	121.7	19	28	Taiwan
101	02-05-72	00-58-21.3	73.4	7.2	33	0	Greenland Sea
102	04-05-72	03-50-28.9	33.5	141.0	45	44	E. Honshu
103	04-05-72	07-48-17.2	-15.9	167.5	45	46	New Hebrides
104	05-05-72	23-16-27.9	- 4.2	152.7	32	37	New Britain-New Ireland
105	06-05-72	17-49-57.0	35.9	141.1	35	46	E. Honshu
106	06-05-72	22-05-19.9	28.3	102.3	14	14	Szechwan
107	07-05-72	06-36-03.0	40.2	78.9	31	40	S. Sinkiang
108	07-05-72	17-20-22.6	-14.9	167.6	31	31	New Hebrides
109	08-05-72	00-07-20.9	73.5	7.6	33	33	Greenland Sea
110	08-05-72	08-58-06.0	40.9	23.5	33	51	Greece-Bulgaria
111	08-05-72	09-20-54.5	41.6	23.5	10	12	Greece-Bulgaria
112	10-05-72	05-10-11.7	- 4.2	150.2	33	33	New Britain-New Ireland
113	10-05-72	05-48-22.0	- 4.1	150.2	33	0	New Britain-New Ireland

TABLE 1 (Cont'd)

Event No.[a]	Date	Origin Time[b]	Lat.(°N)[b,c]	Long.(°E)[b]	Depth (km) NEIC	Depth (km) ISC	Location
114	11-05-72	08-00-06.3	- 4.0	150.1	34	21	New Britain-New Ireland
115	14-05-72	12-01-16.1	40.3	143.4	12	17	E. Honshu
116	16-05-72	10-59-52.6	28.4	52.6	37	45	S. Iran
117	17-05-72	10-06-05.8	33.5	71.5	33	17	Pakistan
118	18-05-72	02-42-17.7	38.6	142.6	39	37	E. Honshu
119	18-05-72	02-42-55.8	27.9	55.8	34	49	S. Iran
120	19-05-72	07-12-45.1	74.0	9.6	33	33	Greenland Sea
121	19-05-72	22-34-00.5	33.8	142.2	37	12	E. Honshu
122	20-05-72	02-34-45.6	-15.6	167.1	33	29	New Hebrides
123	20-05-72	06-44-26.1	28.3	52.8	33	79	S. Iran
124	20-05-72	21-15-52.8	33.6	142.3	16	16	E. Honshu
125	21-05-72	07-57-05.2	73.6	7.6	33	27	Greenland Sea
126	22-05-72	06-04-00.1	16.6	122.3	34	36	Luzon
127	22-05-72	06-11-13.0	16.6	122.5	33	33	Luzon
128	23-05-72	00-19-28.6	16.8	122.4	45	57	Luzon
129	23-05-72	03-14-28.2	41.7	23.6	5	5	Greece-Bulgaria
130	23-05-72	18-03-21.7	33.5	142.3	19	19	E. Honshu
131	23-05-72	18-17-14.1	38.5	70.2	33	54	Tadzhikistan
132	24-05-72	10-12-49.2	13.1	57.6	33	33	Arabian Sea
133	25-05-72	04-12-16.5	23.9	122.2	48	66	Taiwan
134	25-05-72	05-31-51.4	16.4	122.5	36	71	Luzon
135	30-05-72	06-38-16.8	38.3	69.5	35	20	Tadzhikistan
136	03-06-72	02-16-51.1	23.5	125.5	33	33	Ryukyu Isl.
137	05-06-72	11-52-52.7	29.8	70.3	27	38	Pakistan
138	05-06-72	19-00-12.0	86.5	38.9	33	33	Svalbard
139E	07-06-72	01-27-57.1	49.8	78.2	0	0	E. Kazakhstan
140	08-06-72	09-39-21.4	34.1	46.2	18	46	W. Iran
141	10-06-72	11-29-10.9	28.2	66.5	17	17	Pakistan

TABLE 1 (Cont'd)

Event No.[a]	Date	Origin Time[b]	Lat.(^oN)[b,c]	Long.(^oE)[b]	Depth NEIC (km)	Depth ISC (km)	Location
142	12-06-72	13-34-00.7	33.1	46.3	33	34	Iran-Iraq
143	13-06-72	00-55-37.3	33.1	46.3	33	31	Iran-Iraq
144	13-06-72	10-45-05.3	54.9	126.4	33	16	E. Russia
145	14-06-72	00-49-54.4	40.1	51.9	47	39	Caspian Sea
146	14-06-72	04-34-28.1	35.0	46.1	33	47	Iran-Iraq
147	16-06-72	18-57-51.6	36.0	69.2	40	33	Hindu Kush
148	17-06-72	09-02-47.5	48.3	14.5	33	20	Austria
149	19-06-72	18-07-53.4	43.8	151.5	33	33	Kurile Isl.
150	21-06-72	03-44-16.1	80.0	0.9	33	33	Svalbard
151	23-06-72	06-50-11.0	36.7	32.4	33	43	Turkey
152	23-06-72	08-39-35.8	32.9	46.2	40	51	Iran-Iraq
153	24-06-72	07-17-55.5	43.7	16.9	33	33	Yugoslavia
154	24-06-72	21-17-58.3	36.4	69.4	33	52	Hindu Kush
155	25-06-72	07-55-45.3	36.3	69.6	46	53	Hindu Kush
156	27-06-72	06-39-44.4	29.7	70.3	12	11	Pakistan
157	27-06-72	10-48-55.6	29.7	70.3	8	18	Pakistan
158	28-06-72	01-43-56.5	43.0	20.5	33	9	Yugoslavia
159	30-06-72	17-49-33.4	27.2	56.8	33	59	S. Iran

[a]An "E" indicates a presumed underground nuclear explosion.
[b]The values given were determined by the National Earthquake Information Center (NEIC), Boulder, Colorado.
[c]A minus sign indicates South latitude.

TABLE 2. BODY-WAVE (m_b) AND SURFACE-WAVE (M_S) MAGNITUDES OF EVENTS STUDIED

Event No.[a]	m_b(NEIC)[b]	m_b(ISC)[b]	m_b[b,c]	M_S(NEIC)[b]	$M_{S,RZ}$[b,c]	$M_{S,L}$[b,c]
1	5.2(24)	5.1(30)	5.03±0.34(8)	---	4.06±0.29(13)	3.91±0.12(4)
2	4.8(10)	4.7(14)	4.61 0.27(8)	---	4.30 0.29(14)	4.09 0.21(2)
3	5.5(24)	5.4(32)	5.59 0.31(15)	5.4(6)	5.42 0.25(23)	5.12 0.24(6)
4	4.1(5)	4.1(5)	4.26 (1)	---	---	---
5	5.1(13)	5.1(16)	4.95 0.32(15)	---	4.74 (1)	4.53 (1)
6	4.6(7)	4.5(7)	4.66 0.32(7)	---	3.71 0.23(2)	3.59 0.04(2)
7	4.4(3)	---	4.58 0.10(4)	---	3.49 0.26(9)	3.41 0.35(3)
8	4.5(4)	4.5(7)	4.69 0.25(7)	---	3.76 0.29(6)	3.85 (1)
9	4.0(3)	3.9(3)	---	---	3.00 0.16(2)	3.05 0.22(2)
10	4.7(2)	---	3.70 (1)	---	---	---
11	5.2(11)	5.1(18)	4.69 0.44(7)	---	3.74 0.24(8)	3.89 0.18(5)
12	5.3(22)	5.3(36)	5.06 0.30(18)	5.3(2)	5.15 0.32(20)	5.43 0.34(9)
13	5.1(10)	5.1(14)	4.97 0.26(6)	5.3(1)	4.14 0.30(9)	4.02 0.31(6)
14	4.7(9)	4.6(9)	4.53 0.35(12)	---	3.93 0.34(5)	3.95 (1)
15	5.4(22)	5.4(37)	5.64 0.23(11)	5.9(6)	5.90 0.48(19)	5.88 0.21(12)
16	5.0(3)	4.8(9)	4.86 0.25(3)	---	3.79 0.36(6)	---
17	4.9(7)	4.8(10)	4.96 0.17(8)	---	3.85 0.16(7)	3.89 0.22(4)
18	4.1(2)	4.1(3)	---	---	---	---
19	5.2(13)	5.1(27)	5.27 0.37(9)	4.8(1)	4.68 0.37(14)	4.88 0.19(8)
20	4.6(6)	4.6(7)	4.76 0.23(8)	---	4.06 0.23(3)	---
21	4.5(4)	4.3(3)	4.24 (1)	---	2.95 (1)	---
22	4.8(3)	---	3.55 0.30(2)	---	3.19 (1)	3.32 (1)
23	4.3(4)	4.0(3)	---	---	---	---
24	4.6(6)	4.7(8)	4.63 0.21(8)	---	3.95 0.10(4)	3.85 (1)
25	4.5(6)	4.4(6)	4.63 0.42(7)	---	4.04 0.29(7)	4.03 0.09(3)
26	4.7(9)	4.8(9)	4.61 0.43(7)	4.4(1)	4.45 0.32(16)	4.62 0.06(2)
27	5.1(14)	5.1(18)	4.91 0.19(9)	5.0(1)	4.75 0.37(21)	4.51 0.39(3)
28	4.5(2)	---	4.55 0.31(4)	4.2(1)	3.81 0.23(5)	3.93 0.01(2)
29	4.8(7)	4.5(5)	4.70 0.39(9)	---	4.27 0.37(15)	4.05 0.34(3)

TABLE 2 (Cont'd)

Event No.[a]	m_b(NEIC)[b]	m_b(ISC)[b]	m_b[b,c]	M_S(NEIC)[b]	$M_{S,RZ}$[b,c]	$M_{S,L}$[b,c]
30	4.4(4)	4.3(6)	4.24±0.41(3)	---	---	---
31	5.2(11)	5.1(18)	5.01 0.43(9)	---	3.92±0.33(8)	4.18 (1)
32	4.8(1)	---	4.22 0.26(4)	---	3.70 0.32(4)	3.47 (1)
33	4.6(6)	3.9(3)	---	---	---	---
34	4.7(12)	4.4(3)	4.46 0.37(3)	---	3.66 0.33(3)	3.68 (1)
35	4.9(7)	4.3(5)	4.38 0.13(6)	---	---	---
36	4.7(2)	4.6(3)	3.60 (1)	---	3.39 0.24(4)	---
37	4.5(5)	4.4(5)	4.81 0.23(4)	---	3.33 0.34(7)	3.85±0.20(3)
38E	5.5(23)	5.4(41)	5.19 0.42(13)	---	3.39 0.08(2)	---
39	4.9(8)	4.7(6)	4.80 0.31(5)	---	4.05 0.30(5)	---
40	4.6(10)	4.6(12)	4.70 0.36(10)	---	4.49 0.22(15)	4.20 0.26(3)
41	4.8(9)	4.8(15)	4.74 0.31(6)	---	3.97 0.52(12)	---
42	4.7(10)	4.6(10)	4.81 0.31(6)	---	4.00 0.29(6)	4.00 (1)
43	4.8(9)	4.8(13)	4.79 0.21(4)	---	3.51 0.43(7)	---
44	4.0(3)	---	---	---	3.42 (1)	---
45	5.4(22)	5.4(44)	5.43 0.36(7)	---	4.54 0.35(14)	4.50 0.32(5)
46	4.7(3)	4.5(3)	4.73 0.31(5)	---	3.75 0.27(6)	---
47	5.3(28)	5.3(36)	5.17 0.32(10)	4.6(1)	4.98 0.32(19)	5.02 0.17(5)
48	4.9(14)	4.8(15)	4.69 0.23(9)	4.8(1)	4.51 0.27(18)	4.34 0.27(18)
49	4.1(3)	4.1(3)	3.92 0.10(2)	---	2.93 0.12(3)	3.07 (1)
50	4.7(6)	4.5(4)	3.97 0.23(4)	---	3.99 0.13(2)	3.93 0.05(2)
51	4.8(4)	4.8(5)	4.87 0.04(3)	---	4.26 0.14(6)	4.31 0.28(4)
52	4.9(3)	4.3(3)	4.58 0.36(2)	---	4.25 0.25(7)	4.37 0.16(4)
53	4.5(6)	4.3(3)	4.74 0.38(6)	---	4.09 0.36(7)	---
54	4.9(9)	4.7(8)	4.46 0.41(5)	---	3.17 (1)	---
55	4.4(2)	---	4.53 0.40(6)	---	3.20 0.35(2)	---
56	4.5(2)	---	4.31 0.18(2)	---	3.86 0.19(6)	---
57	5.0(8)	5.0(14)	5.19 0.36(6)	---	4.98 0.26(17)	4.69 0.39(6)
58	4.9(6)	4.6(7)	4.52 0.62(4)	---	3.98 0.14(9)	4.29 (1)

TABLE 2 (Cont'd)

Event No.[a]	m_b(NEIC)[b]	m_b(ISC)[b]	m_b[b,c]	M_S(NEIC)[b]	$M_{S,RZ}$[b,c]	$M_{S,L}$[b,c]
59E	5.5(39)	5.4(54)	5.31±0.26(13)	---	3.62±0.27(5)	---
60	4.9(12)	4.9(16)	5.06 0.31(4)	---	4.23 0.42(9)	3.40 (1)
61	4.9(10)	5.0(14)	4.86 0.14(5)	---	4.81 0.31(19)	4.62±0.20(5)
62	5.3(19)	5.1(25)	5.07 0.40(7)	---	4.07 0.23(10)	4.20 (1)
63	4.9(12)	4.9(16)	4.77 0.40(7)	---	4.34 0.29(13)	4.34 0.21(2)
64	5.2(23)	5.1(35)	4.95 0.26(9)	---	4.74 0.27(21)	---
65	4.3(3)	4.2(3)	4.54 0.15(3)	---	4.08 0.45(9)	4.33 0.51(3)
66	4.9(7)	4.9(15)	4.72 0.45(13)	---	4.33 0.29(17)	4.25 0.49(3)
67	4.6(7)	4.5(7)	4.55 0.44(9)	---	4.30 0.26(15)	4.08 0.26(2)
68	4.8(9)	4.6(14)	4.77 0.35(8)	---	4.30 0.33(21)	3.42 (1)
69	5.2(22)	5.2(30)	4.97 0.27(13)	4.4(1)	4.54 0.26(23)	4.39 0.23(2)
70	5.0(9)	4.9(13)	4.94 0.14(5)	---	4.18 0.36(12)	4.69 (1)
71	5.4(16)	5.3(28)	5.08 0.37(15)	4.6(1)	4.81 0.24(21)	4.52 0.30(3)
72	4.8(7)	4.7(7)	4.37 0.45(6)	---	3.63 0.27(7)	---
73	4.5(5)	4.4(4)	4.63 0.07(2)	---	3.33 0.25(3)	---
74E	5.2(23)	5.1(35)	4.89 0.31(7)	---	3.45 0.14(3)	---
75	5.0(13)	4.9(22)	4.68 0.37(6)	---	4.25 0.37(11)	4.34 (1)
76	4.7(5)	4.5(5)	4.60 0.59(4)	---	3.36 0.09(2)	---
77	4.8(6)	4.6(9)	4.36 0.44(9)	---	3.52 0.62(7)	---
78	4.8(2)	---	4.37 0.21(4)	---	3.35 0.13(4)	---
79	4.8(9)	4.7(11)	4.49 0.41(10)	---	3.20 (1)	---
80	4.9(5)	4.5(5)	4.54 0.21(5)	---	3.85 0.41(6)	---
81	6.1(36)	6.0(55)	5.79 0.20(4)	6.9(9)	6.72 0.17(5)	6.61 (1)
82	4.9(5)	4.7(1)	4.65 0.15(4)	---	---	---
83	4.7(8)	4.8(13)	4.56 0.30(6)	---	3.72 0.17(6)	---
84	4.9(8)	4.9(16)	4.70 0.25(6)	---	4.02 0.54(11)	---
85	4.6(1)	4.7(3)	4.46 0.44(3)	---	3.59 0.33(10)	---
86	5.1(16)	4.9(23)	4.77 0.08(3)	---	3.85 0.12(4)	---
87	4.9(9)	4.7(8)	4.49 0.36(13)	---	4.50 0.34(19)	4.38 0.36(2)

TABLE 2 (Cont'd)

Event No.[a]	m_b(NEIC)[b]	m_b(ISC)[b]	m_b[b,c]	M_S(NEIC)[b]	$M_{S,RZ}$[b,c]	$M_{S,L}$[b,c]
88	4.8(7)	4.8(4)	4.60±0.29(5)	---	3.66±0.17(4)	---
89	5.1(15)	4.6(18)	4.75 0.45(8)	---	---	---
90	4.8(10)	4.7(12)	4.43 0.38(7)	---	4.05 0.40(10)	3.50 (1)
91	5.1(15)	5.0(22)	4.63 0.30(10)	---	3.89 0.41(13)	---
92	4.8(10)	4.8(16)	4.89 0.25(7)	---	3.93 0.30(11)	4.10±0.13(3)
93	4.8(5)	4.7(5)	4.28 0.36(4)	---	3.96 0.36(10)	3.42 0.19(3)
94	6.2(30)	6.4(47)	---	7.2(9)	---	---
95	5.2(11)	5.2(15)	4.86 0.39(8)	5.2(2)	5.19 0.29(5)	4.81 0.14(2)
96	5.0(1)	---	4.49 0.26(7)	---	4.07 0.16(11)	3.88 0.46(7)
97	4.7(2)	---	4.52 0.32(6)	---	3.92 0.36(6)	3.38 (1)
98	5.1(11)	5.0(16)	5.16 0.16(4)	---	4.26 0.31(11)	4.17 0.05(5)
99	5.2(10)	5.2(7)	4.90 0.43(10)	---	4.31 0.29(13)	4.09 0.19(7)
100	4.7(1)	4.8(3)	4.29 0.12(5)	---	4.06 0.31(5)	4.48 0.21(4)
101	5.0(4)	4.5(6)	4.30 0.14(3)	---	3.46 0.06(6)	3.48 0.07(4)
102	5.5(12)	5.4(32)	5.19 0.28(6)	---	4.91 0.37(26)	5.01 0.50(3)
103	6.1(14)	6.3(28)	6.26 0.40(4)	6.8(5)	6.72 0.29(14)	6.37 0.10(10)
104	5.6(9)	5.8(13)	5.62 0.35(7)	6.6(6)	6.50 0.20(16)	6.28 0.18(10)
105	4.7(3)	4.6(4)	4.23 0.17(4)	---	3.70 0.44(5)	---
106	4.9(2)	4.8(6)	4.36 0.27(4)	---	3.51 0.30(8)	3.44 0.31(7)
107	4.8(2)	4.7(3)	4.23 0.38(5)	---	3.48 0.49(6)	3.69 0.02(2)
108	5.2(5)	5.2(7)	4.49 0.09(3)	---	---	---
109	4.5(2)	4.3(4)	≤3.8	---	---	---
110	4.5(1)	---	≤4.0	---	2.98 0.21(5)	---
111	5.0(14)	4.9(16)	4.47 0.43(7)	---	3.59 0.32(8)	3.54 0.24(2)
112	5.0(6)	4.9(6)	4.86 0.36(7)	---	4.41 0.33(17)	4.12 0.30(5)
113	5.5(8)	5.5(11)	5.37 0.25(7)	5.2(1)	5.36 0.32(26)	5.12 0.23(16)

TABLE 2 (Cont'd)

Event No.[a]	m_b(NEIC)[b]	m_b(ISC)[b]	m_b[b,c]	M_S(NEIC)[b]	$M_{S,RZ}$[b,c]	$M_{S,L}$[b,c]
114	5.0(6)	5.0(6)	4.79±0.35(6)	---	4.52±0.38(9)	4.11±0.42(4)
115	5.3(12)	5.2(28)	5.23 0.46(8)	---	5.27 0.36(18)	4.82 0.40(3)
116	5.0(7)	4.8(17)	4.66 0.10(4)	---	3.61 0.21(10)	3.84 0.36(4)
117	5.3(5)	5.0(17)	4.87 0.46(6)	---	4.31 0.28(7)	4.20 0.21(5)
118	---	---	---	---	---	---
119	4.6(5)	4.7(8)	4.34 0.33(4)	---	3.84 0.22(10)	3.78 0.15(5)
120	4.8(3)	3.9(4)	3.82 0.17(2)	---	3.32 0.03(2)	3.18 0.00(2)
121	4.2(1)	4.6(3)	4.68 0.41(4)	---	3.70 0.17(5)	---
122	5.2(5)	5.2(6)	4.83 0.20(3)	5.5(3)	5.46 0.30(17)	5.02 0.20(11)
123	4.9(3)	4.8(5)	4.00 0.28(2)	---	3.06 0.17(4)	3.08 0.19(4)
124	4.5(2)	4.8(8)	4.78 0.57(4)	---	3.87 0.51(6)	---
125	4.5(8)	4.3(8)	4.45 0.30(7)	---	3.55 0.54(4)	3.38 0.17(2)
126	5.7(15)	5.9(37)	5.98 0.14(5)	6.9(5)	6.76 0.33(12)	6.39 0.33(5)
127	5.3(5)	5.5(11)	5.41 0.33(6)	---	---	---
128	5.0(4)	4.9(7)	4.96 0.35(5)	---	4.11 0.16(4)	3.92 0.06(2)
129	4.3(2)	4.4(3)	≤ 4.0	---	≤ 2.8	---
130	5.1(9)	5.1(17)	4.98 0.48(8)	---	3.99 0.29(12)	---
131	4.9(4)	4.7(8)	4.40 0.38(5)	---	3.45 0.12(4)	3.39 (1)
132	4.7(7)	4.2(4)	4.50 0.33(5)	---	3.83 0.27(14)	3.86 (1)
133	5.2(2)	---	4.47 0.29(3)	---	3.56 0.38(6)	3.85 0.38(4)
134	5.1(1)	---	4.30 0.27(3)	---	3.58 0.38(10)	3.88 0.28(5)
135	5.1(8)	4.9(12)	4.75 0.44(5)	---	3.39 0.21(4)	3.97 (1)
136	5.2(7)	4.9(9)	4.72 0.56(7)	---	4.19 0.30(21)	3.68 0.16(4)
137	4.8(1)	---	4.08 0.17(4)	---	3.31 0.45(6)	---
138	4.4(4)	4.2(5)	4.23 0.39(12)	---	3.79 0.34(19)	---
139E	5.5(14)	5.4(42)	5.07 0.34(13)	---	3.43 0.36(8)	---
140	4.9(8)	4.9(18)	4.95 0.15(6)	---	4.14 0.03(2)	4.51 (1)
141	4.5(1)	---	4.59 0.16(5)	---	3.81 0.47(12)	4.17 (1)

TABLE 2 (Cont'd)

Event No.[a]	m_b(NEIC)[b]	m_b(ISC)[b]	m_b[b,c]	M_S(NEIC)[b]	$M_{S,RZ}$[b,c]	$M_{S,L}$[b,c]
142	5.4(22)	5.3(38)	5.32±0.31(8)	5.0(1)	4.86±0.44(11)	4.85±0.41(3)
143	5.1(15)	5.0(33)	5.08 0.21(8)	---	4.49 0.36(19)	4.55 0.47(6)
144	4.8(10)	4.9(21)	4.86 0.40(14)	5.4(2)	4.79 0.29(18)	4.86 (1)
145	4.7(8)	4.7(12)	4.80 0.15(4)	---	3.37 0.55(7)	---
146	5.3(18)	5.2(34)	5.25 0.18(7)	---	4.11 0.58(13)	4.15 0.35(2)
147	4.5(5)	4.4(5)	4.75 0.31(5)	---	3.59 0.30(10)	---
148	4.6(6)	---	4.08 0.36(11)	---	2.73 0.09(2)	---
149	4.5(5)	4.4(6)	4.65 0.35(12)	---	3.79 0.27(12)	---
150	4.3(7)	4.4(6)	4.39 0.29(9)	---	3.72 0.34(15)	4.09 0.16(2)
151	4.3(3)	---	4.35 0.32(3)	---	3.48 0.32(4)	---
152	4.6(4)	4.7(7)	4.51 0.26(4)	---	3.81 0.35(9)	3.82 0.52(3)
153	5.3(7)	---	4.17 0.31(10)	---	3.10 0.21(5)	3.20 0.13(3)
154	4.6(1)	---	4.33 0.42(4)	---	3.56 0.57(13)	---
155	4.7(11)	4.8(22)	4.98 0.45(11)	---	4.30 0.22(16)	4.38 (1)
156	5.5(8)	5.1(20)	4.90 0.29(6)	---	4.20 0.45(18)	4.05 0.71(2)
157	5.4(5)	5.0(16)	4.97 0.32(6)	---	4.24 0.51(7)	3.93 (1)
158	4.9(7)	3.9(3)	3.95 0.28(5)	---	3.16 0.42(6)	---
159	4.6(5)	4.4(11)	4.62 0.28(6)	---	3.81 0.23(13)	3.57 (1)

[a]The hypocentral coordinates of each event are given in Table 1.
[b]The numbers in parentheses indicate the number of stations whose data were used.
[c]The number following the "±" sign is the standard deviation.

TABLE 3. ANOMALOUS EARTHQUAKES

Event No.	Location	$M_{S,RZ}$	$M_{S,L}$	Anomalous if using m_b value of NEIC	ISC	This report
1	S. Sinkiang	4.06	3.91	*	*	
11	Iran	3.74	3.89	*	*	
16	S. Sinkiang	5.90	5.88	*		
21	Central Italy	2.95	-	*	*	
22	Central Italy	3.19	3.22	*		
31	Tibet	3.92	4.18	*	*	
36	S. Sinkiang	3.39	-	*		
37	E. Caucasus	3.33	3.85			*
43	Tibet	3.52	-	*	*	*
45	Andaman Isl.	4.54	4.50	*	*	*
54	Yugoslavia	3.17	-	*	*	
55	S. Sinkiang	3.20	-			*
62	Tibet	4.07	4.20	*		
73	E. India	3.33				*
76	Kirgiziya-Sinkiang	3.36	-	*		
77	N. Sinkiang	3.52	-	*		
78	Tibet	3.35	-	*		
79	S. Sinkiang	3.20	-	*	*	
86	S. Iran	3.85	-	*		
91	N. Sinkiang	3.89	-	*	*	
101	Greenland Sea	3.46	3.48	*		
102	E. Honshu	4.91	5.01	*		
103	New Hebrides	6.72	6.37		*	*
106	Szechwan	3.51	3.44	*	*	
107	S. Sinkiang	3.48	3.69	*		

TABLE 3 (Cont'd)

Event No.	Location	$M_{S,RZ}$	$M_{S,L}$	Anomalous if using m_b value of NEIC	ISC	This report
110	Greece-Bulgaria	2.98	-	*		
111	Greece-Bulgaria	3.59	3.54	*	*	
116	S. Iran	3.61	3.84	*		
117	Pakistan	4.31	4.20	*		
120	Greenland Sea	3.32	3.18	*		
123	S. Iran	3.06	3.08	*	*	
129	Greece-Bulgaria	≤2.8	-		*	
130	E. Honshu	3.99	-	*	*	
131	Tadzhikistan	3.45	3.39	*		
133	Taiwan	3.56	3.85	*		
134	Luzon	3.58	3.88	*		
135	Tadzhikistan	3.39	3.97	*	*	*
136	Ryukyu Isl.	4.19	3.68	*		
137	Pakistan	3.31	-	*		
145	Caspian Sea	3.37	-	*	*	*
146	Iran-Iraq	4.11	4.15	*	*	*
148	Austria	2.73	-	*		*
156	Pakistan	4.20	4.05	*		
157	Pakistan	4.24	3.93	*		
158	Yugoslavia	3.16	-	*		

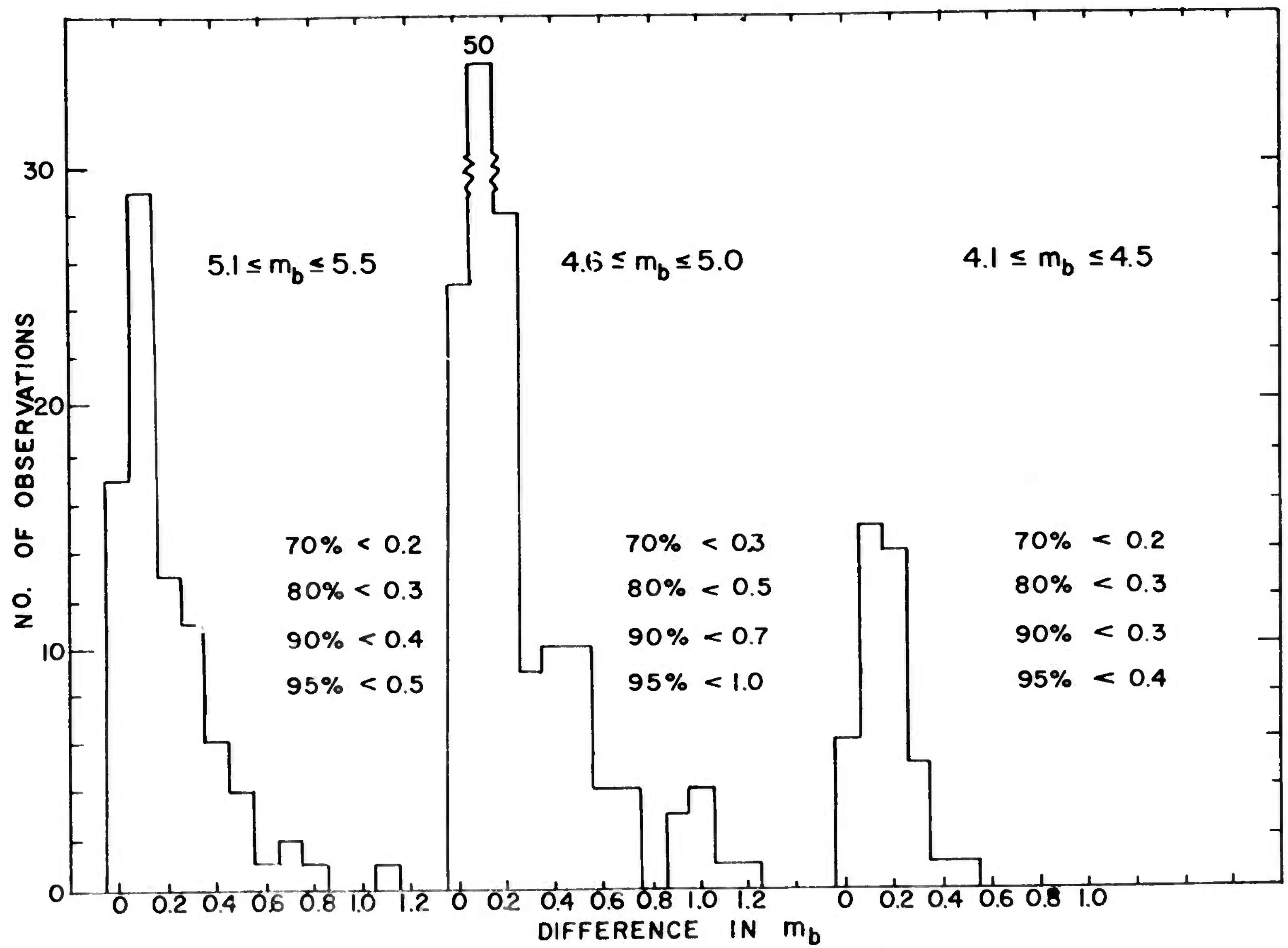

Figure 1. Histograms of the absolute value of the difference between the NEIC m_b and those of the ISC and of the present study, for three different NEIC m_b intervals.

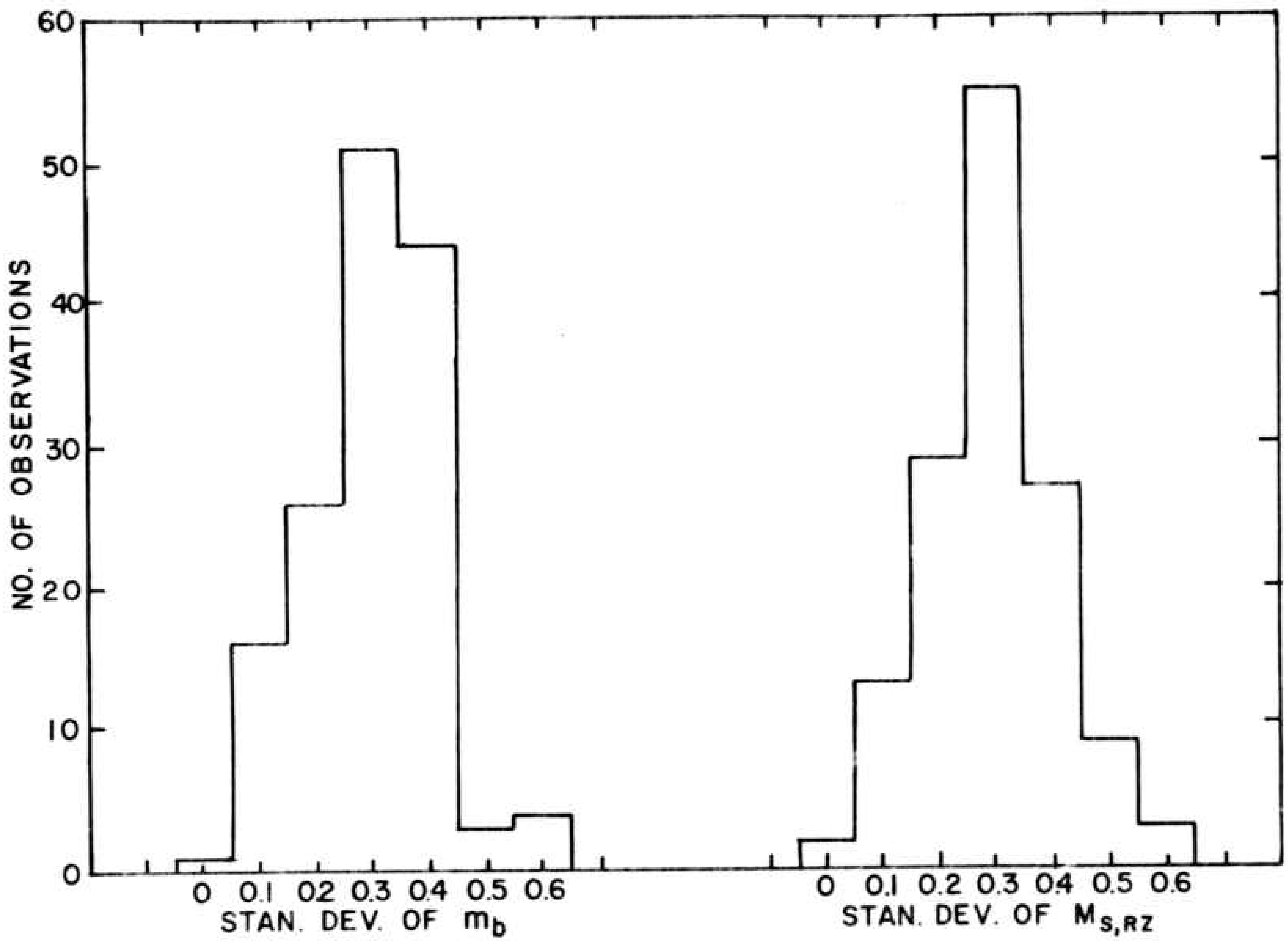

Figure 2. Histograms of the standard deviations of the m_b and $M_{S,RZ}$ values.

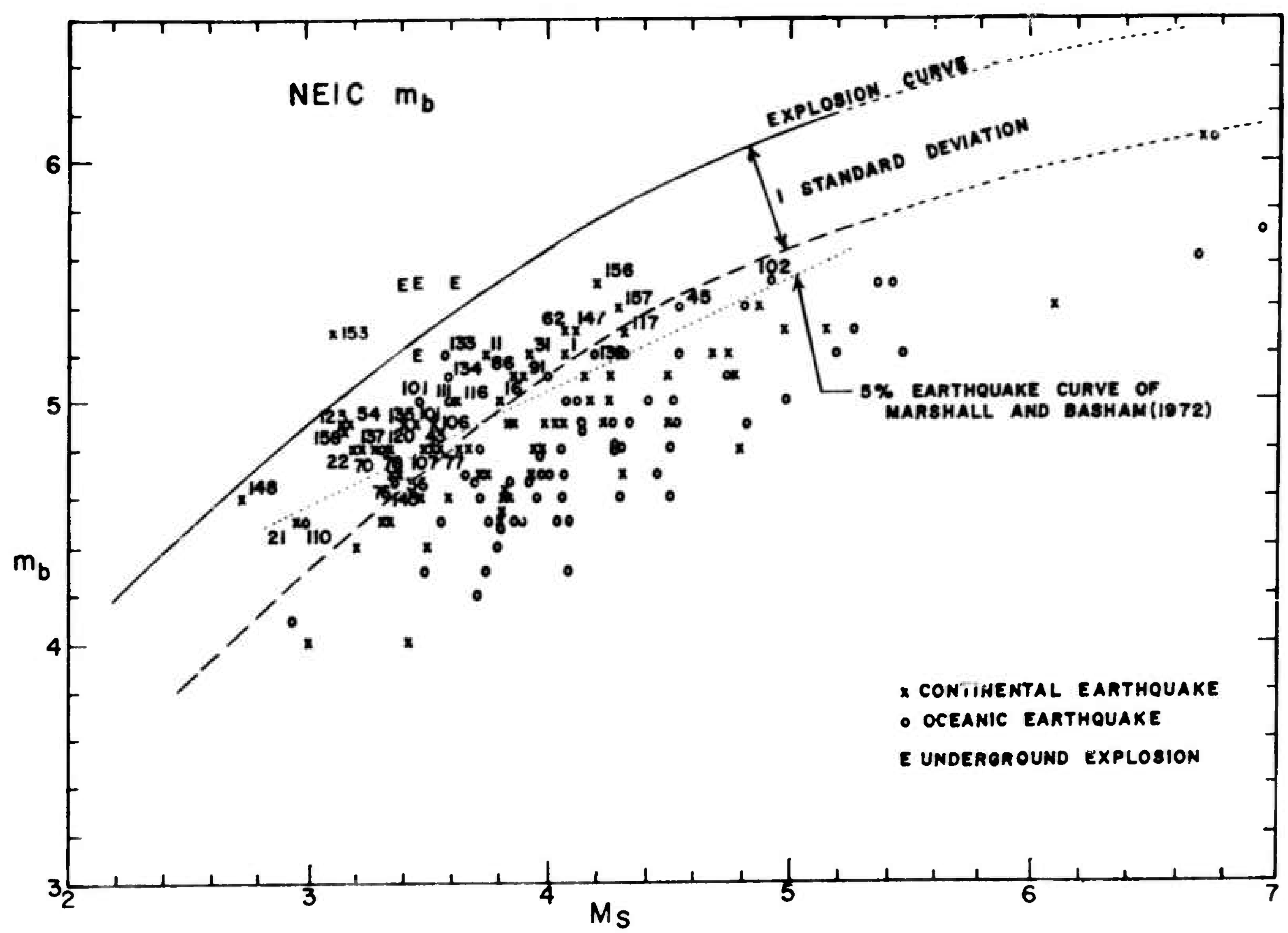

Figure 3. m_b vs M_S values for the 159 events studied, using NEIC m_b values.

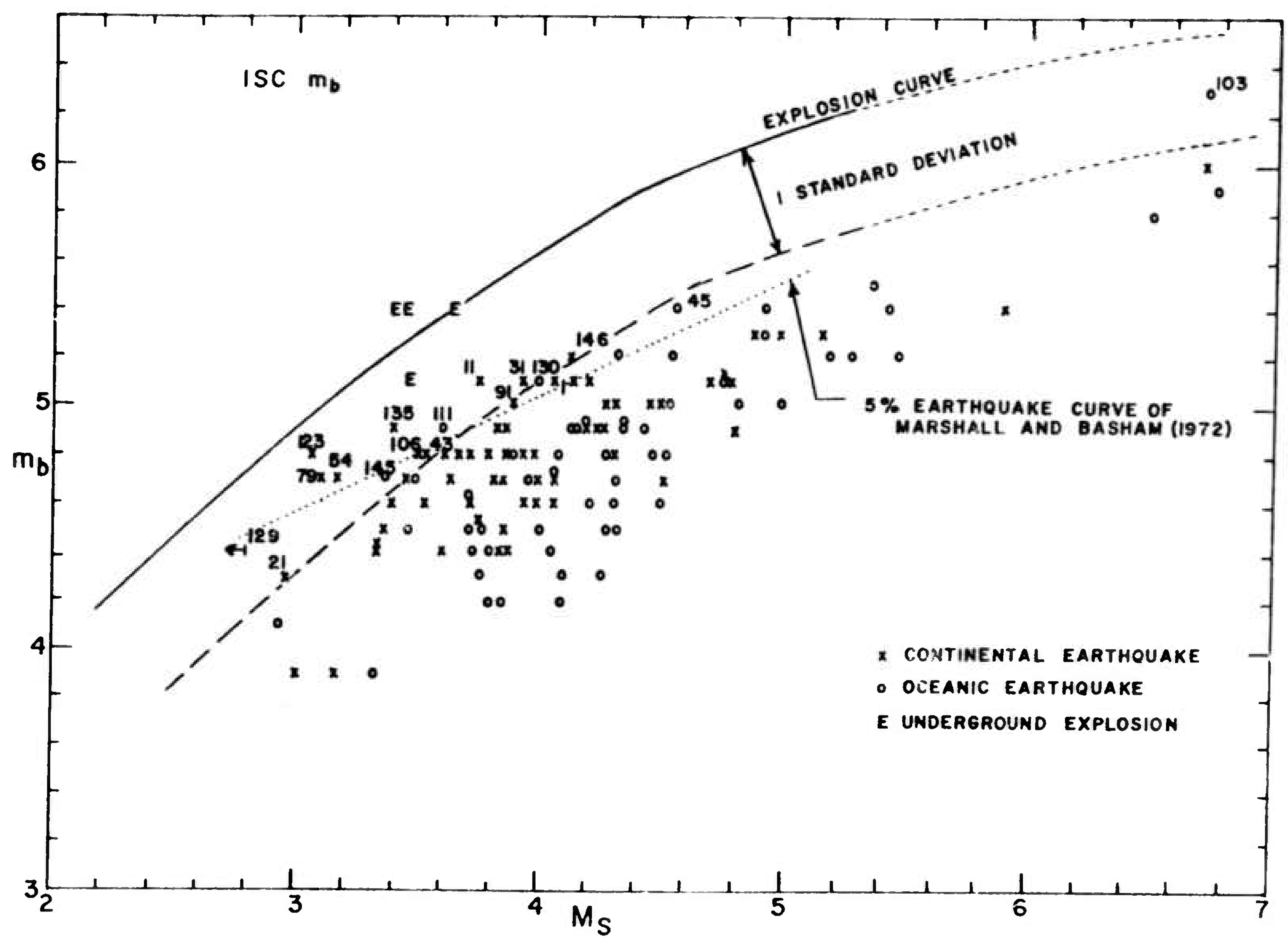

Figure 4. m_b vs M_S values for the 159 events studied, using ISC m_b values.

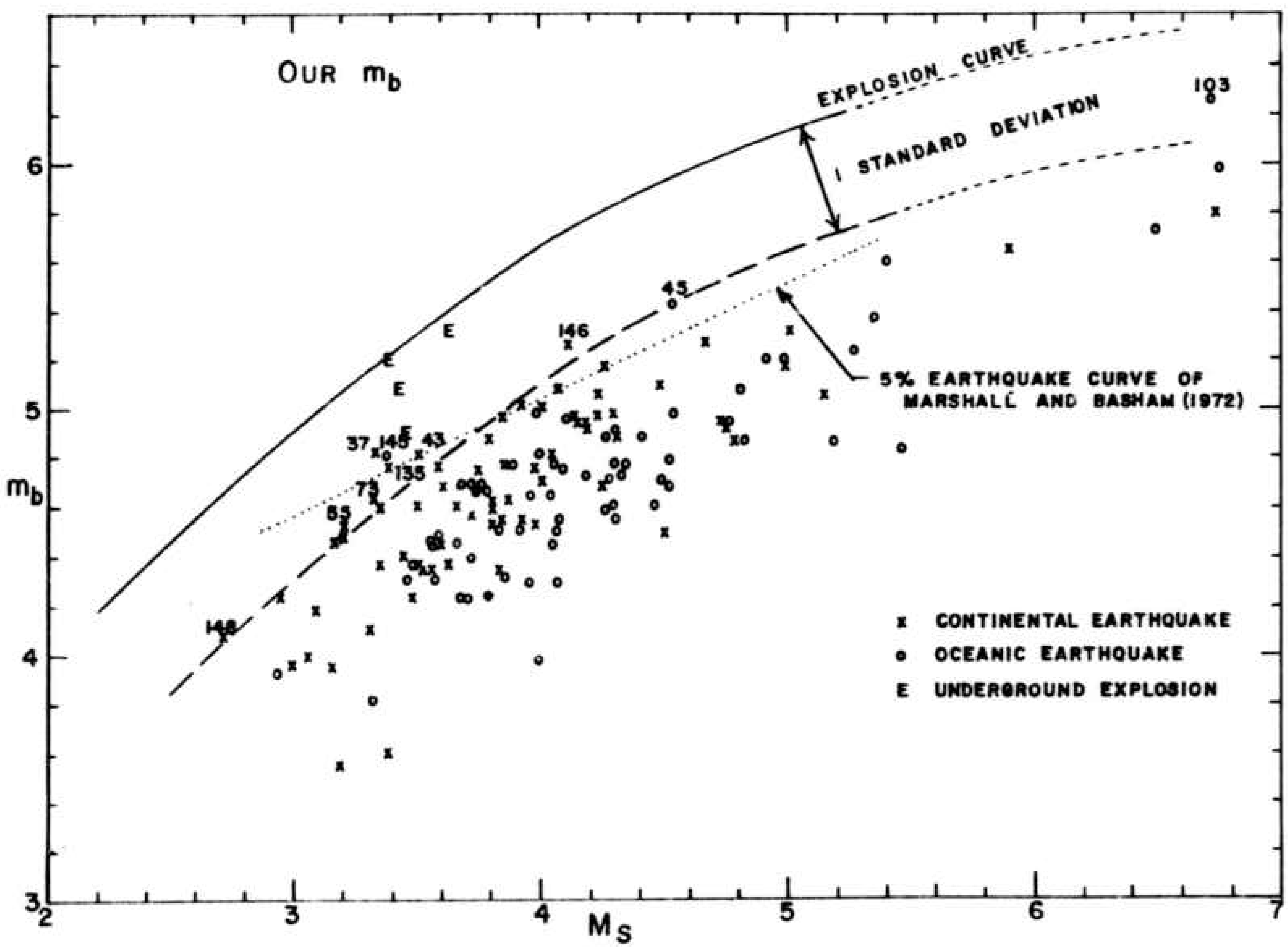

Figure 5. m_b vs M_S values for the 159 events studied, using our m_b values.

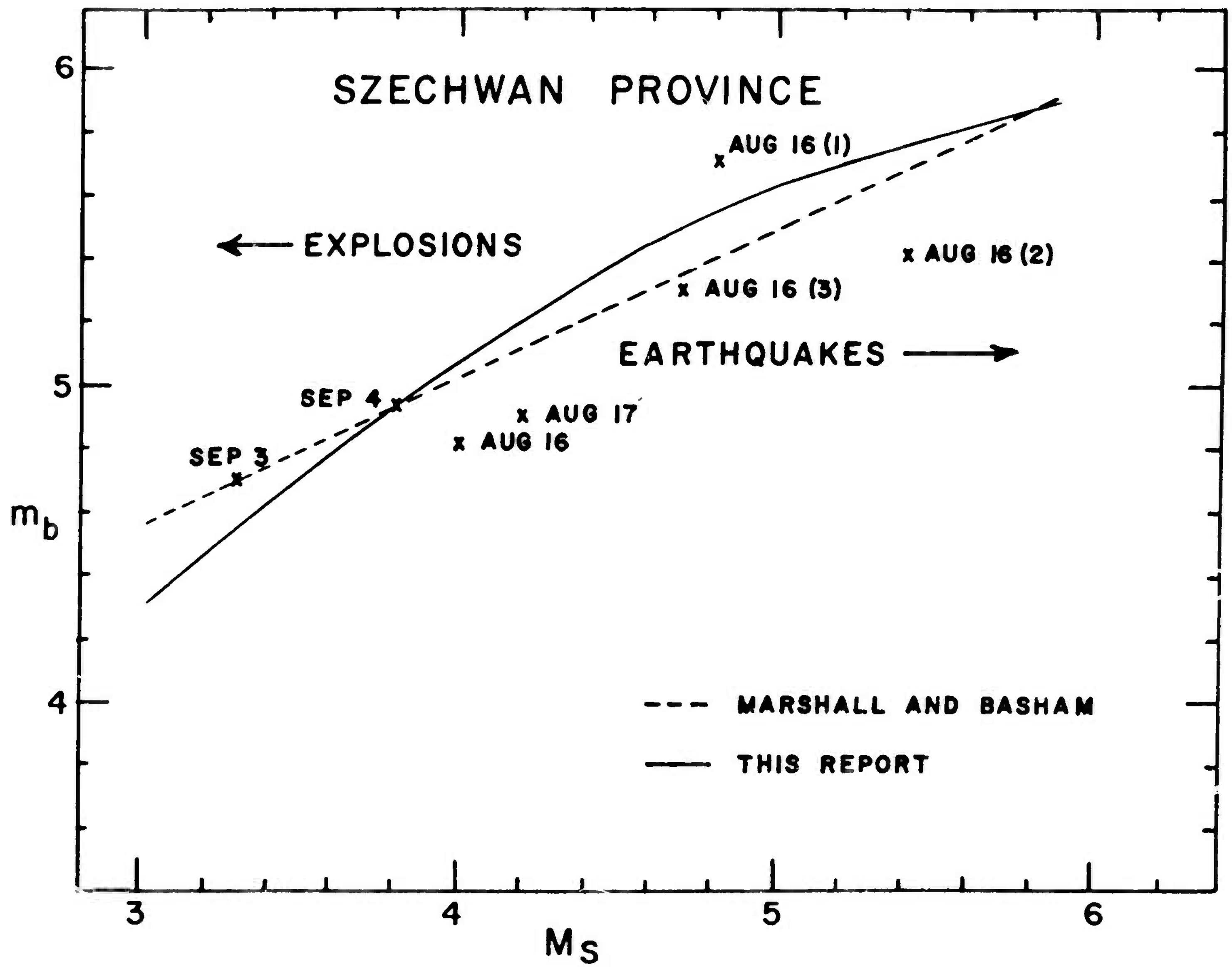

Figure 6. m_b vs M_S values for Szechwan, China aftershock sequence of August-September 1971.

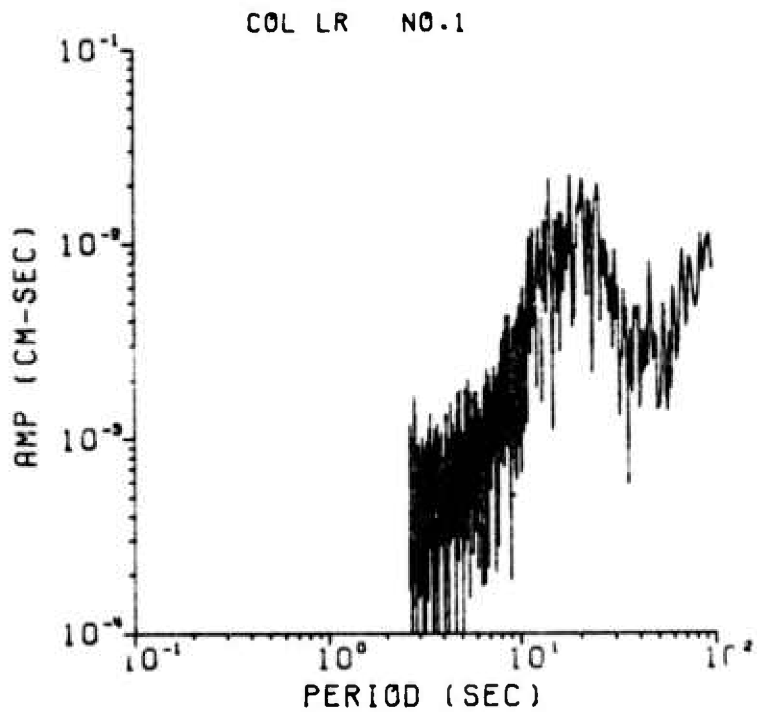

Figure 7a. Vertical-component Rayleigh-wave spectrum for earthquake 1 of 16 August 1971 as recorded at College, Alaska.

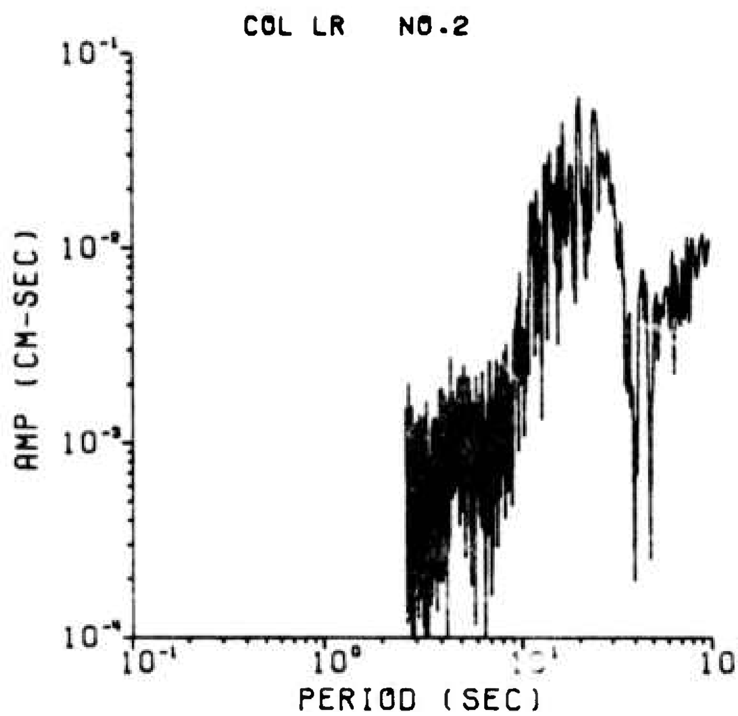

Figure 7b. Vertical-component Rayleigh-wave spectrum for earthquake 2 of 16 August 1971 as recorded at College, Alaska.

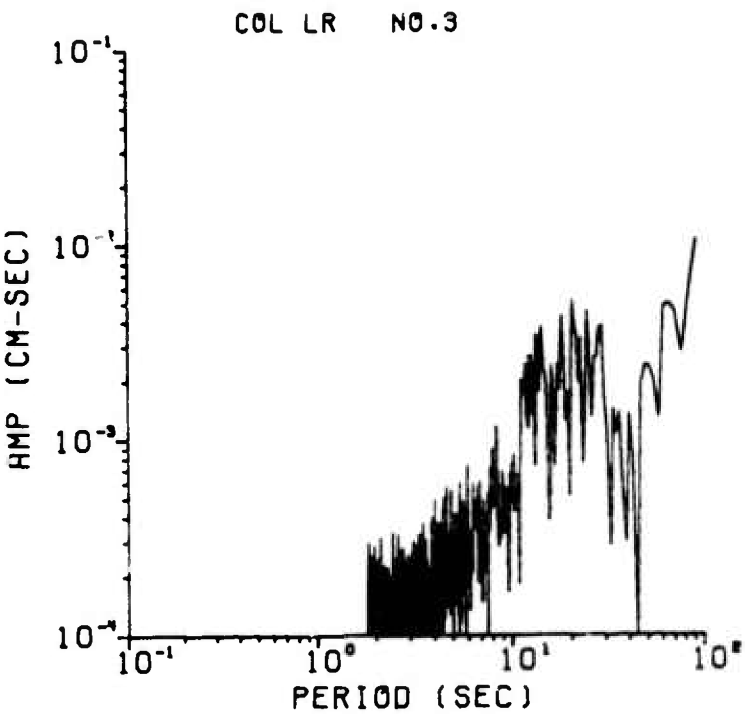

Figure 7c. Vertical-component Rayleigh-wave spectrum for earthquake 3 of 16 August 1971 as recorded at College, Alaska.

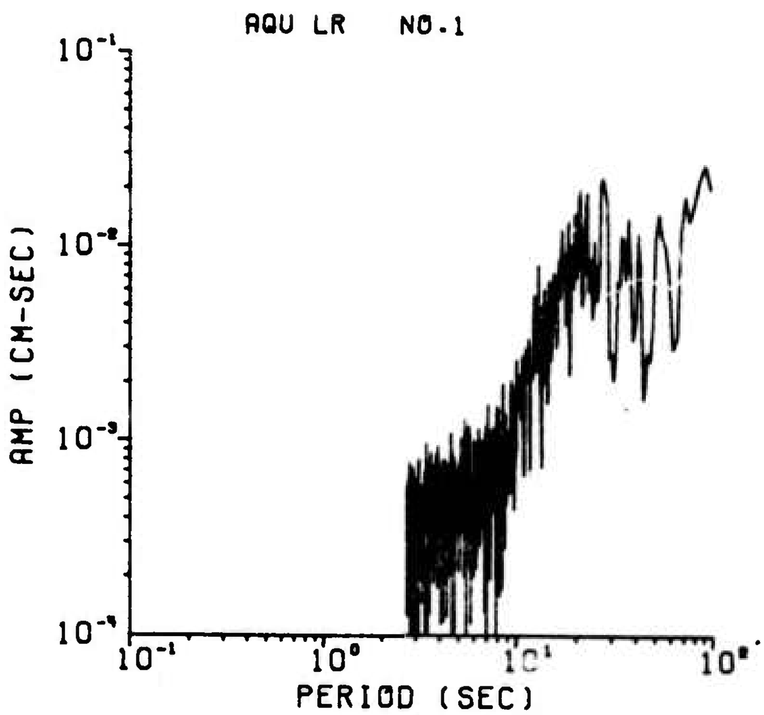

Figure 8a. Vertical-component Rayleigh-wave spectrum for earthquake 1 of 16 August 1971 as recorded at Aquila, Italy.

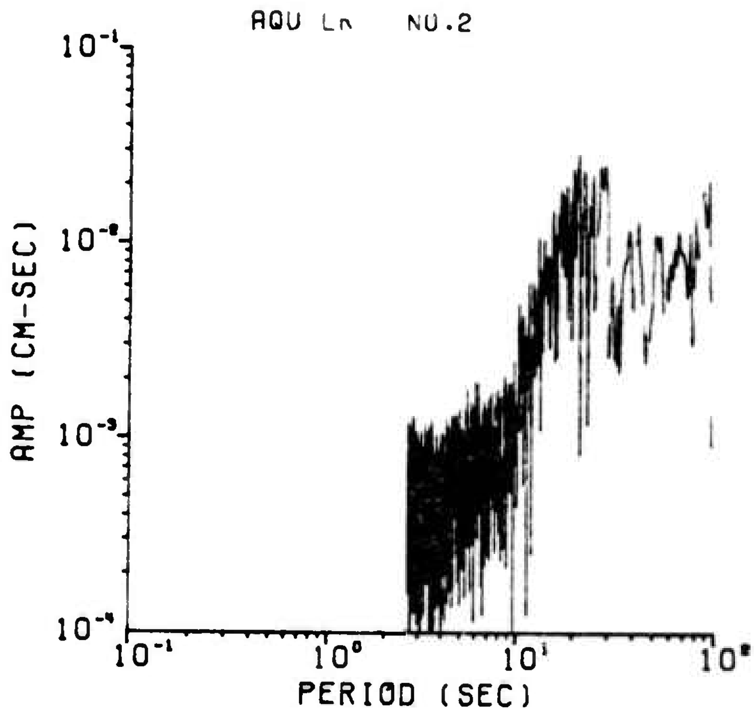

Figure 8b. Vertical-component Rayleigh-wave spectrum for earthquake 2 of 16 August 1971 as recorded at Aquila, Italy.

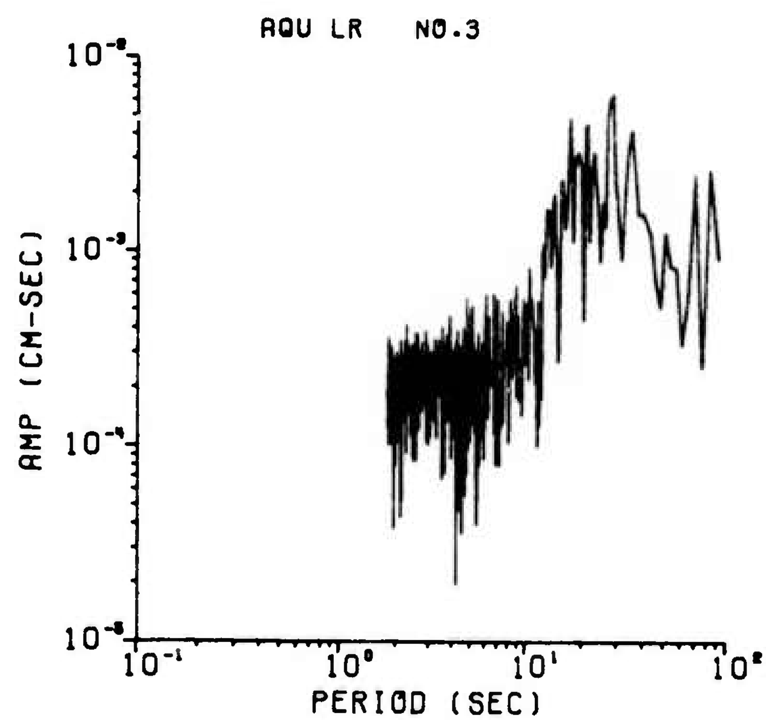

Figure 8c. Vertical-component Rayleigh-wave spectrum for earthquake 3 of 16 August 1971 as recorded at Aquila, Italy.

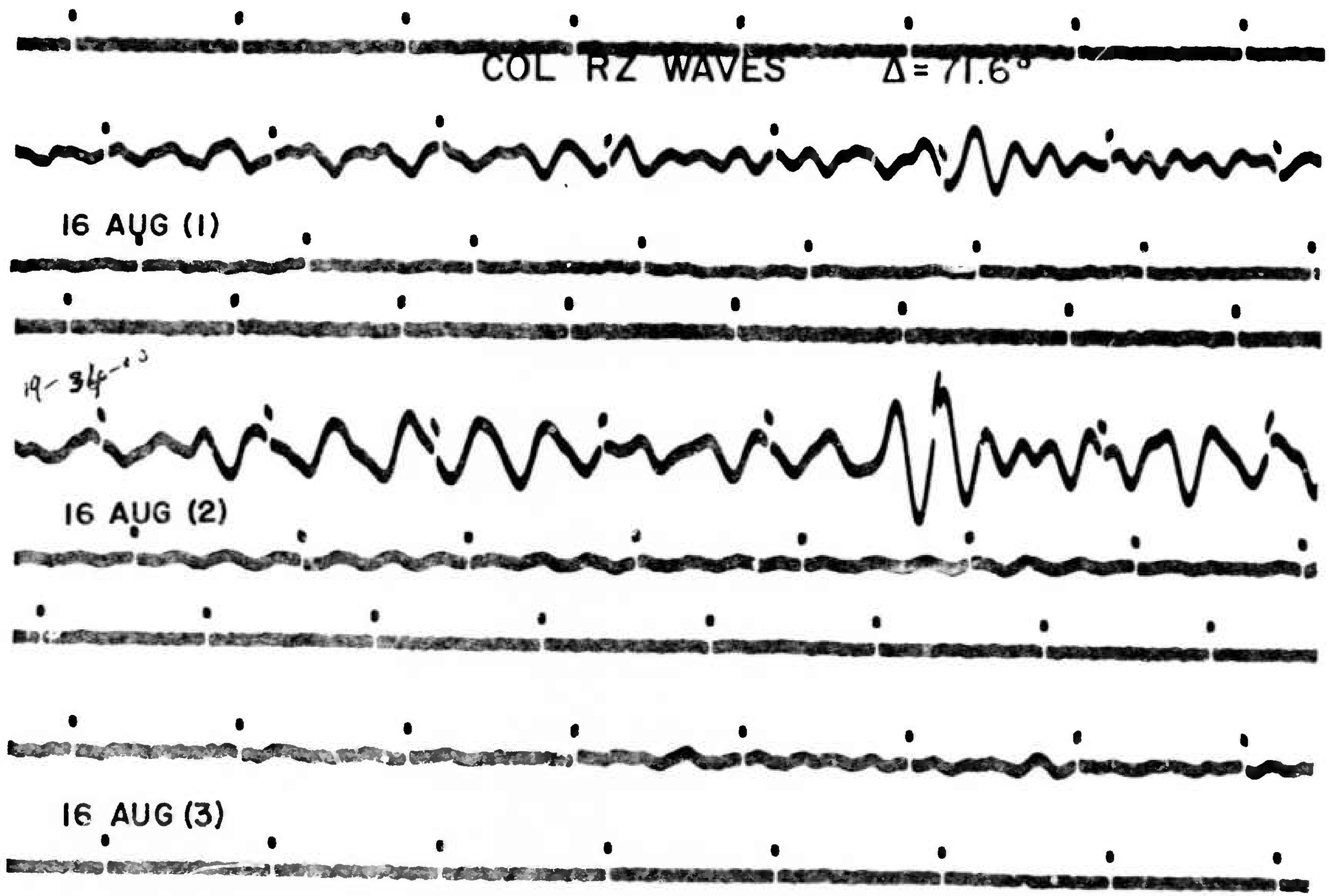

Figure 9. Vertical-component Rayleigh waves for earthquakes of 16 August 1971 as recorded at College, Alaska.

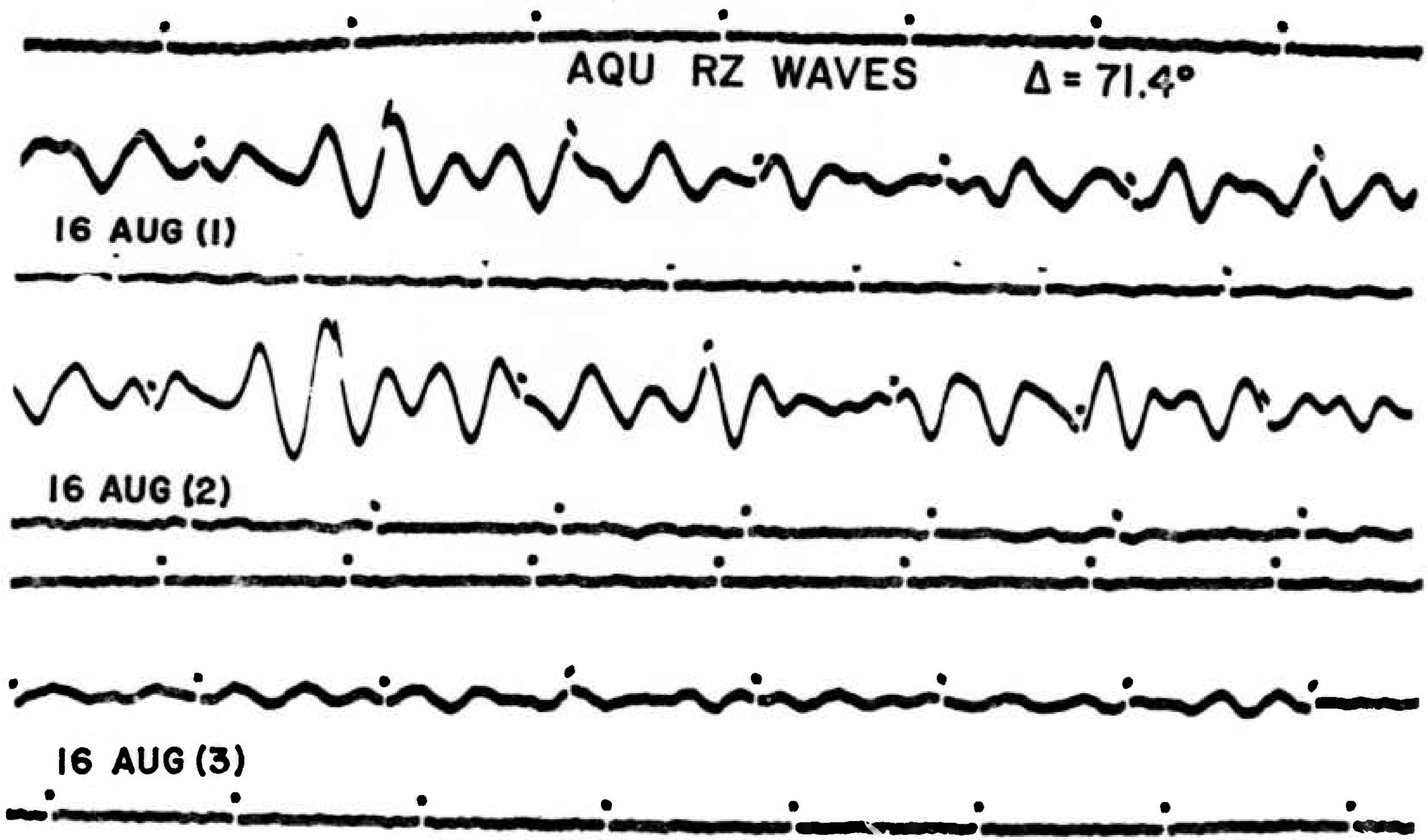

Figure 10. Vertical-component Rayleigh waves for earthquakes of 16 August 1971 as recorded at Aquila, Italy.

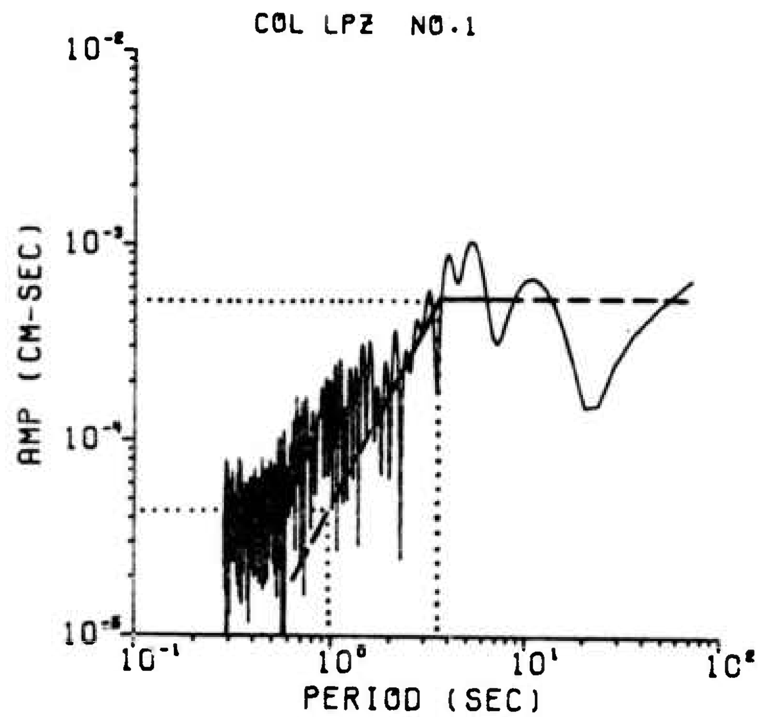

Figure 11a. Spectrum of vertical component of P-wave motion from long-period seismogram for earthquake 1 of 16 August 1971, as recorded at College, Alaska.

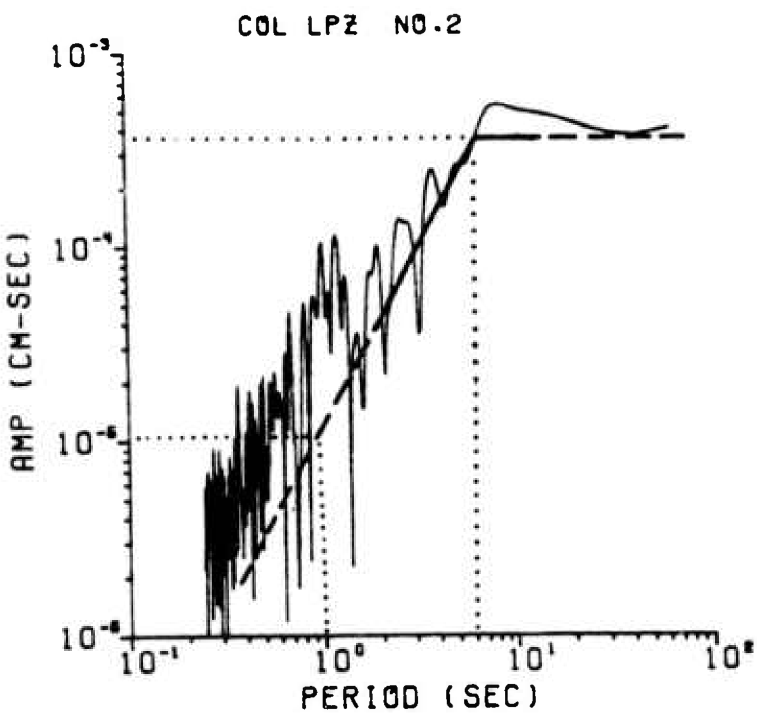

Figure 11b. Spectrum of vertical component of P-wave motion from long-period seismogram for earthquake 2 of 16 August 1971, as recorded at College, Alaska.

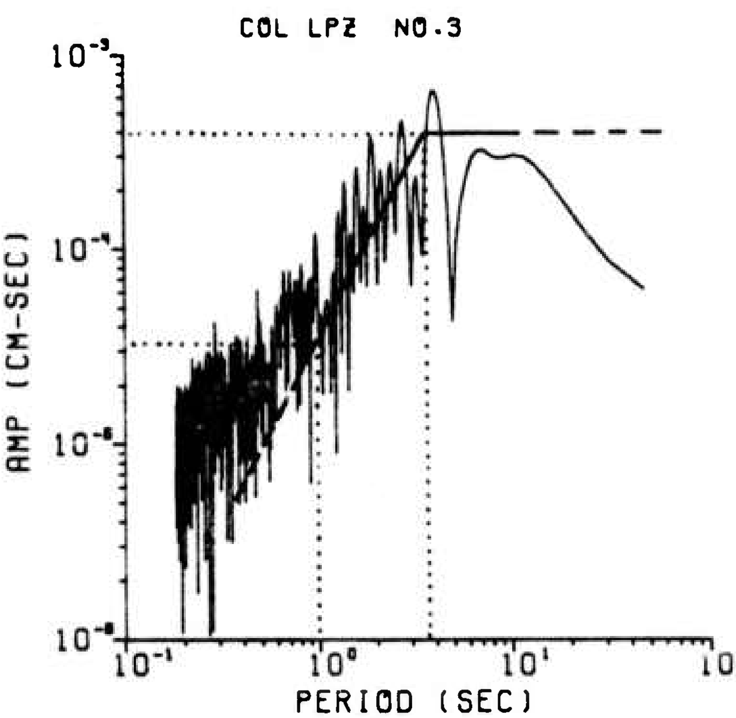

Figure 11c. Spectrum of vertical component of P-wave motion from long-period seismogram for earthquake 3 of 16 August 1971, as recorded at College, Alaska.

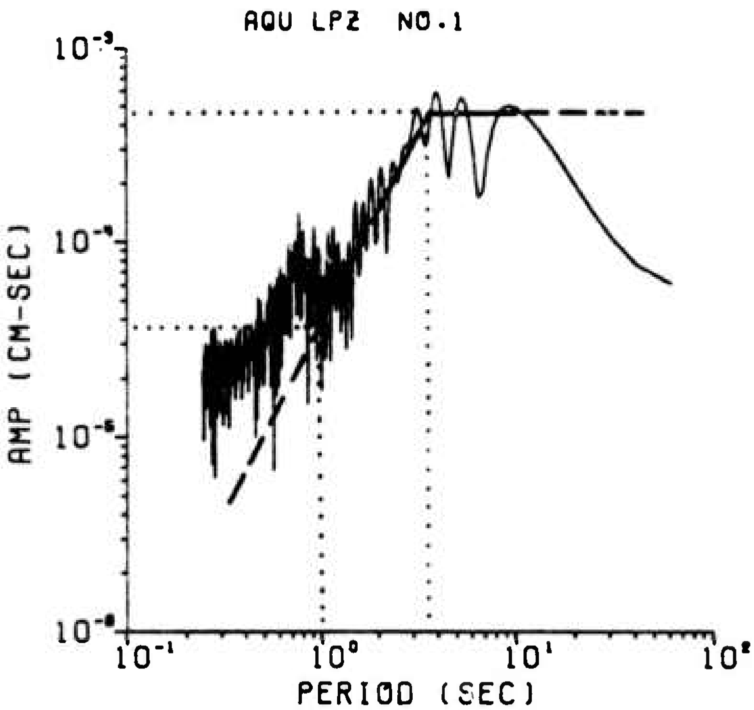

Figure 12a. Spectrum of vertical component of P-wave motion from long-period seismogram for earthquake 1 of 16 August 1971, as recorded at Aquila, Italy.

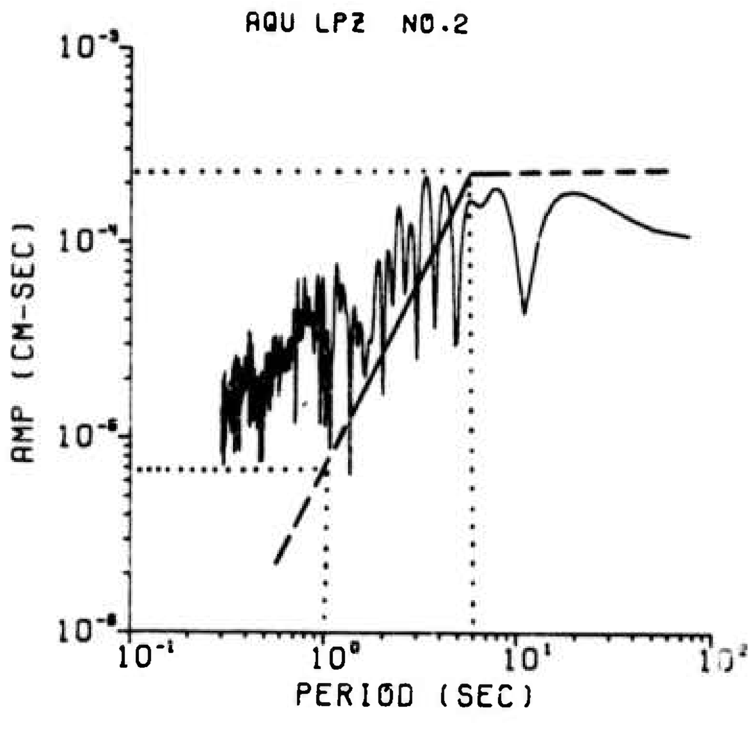

Figure 12b. Spectrum of vertical component of P-wave motion from long-period seismogram for earthquake 2 of 16 August 1971, as recorded at Aquila, Italy.

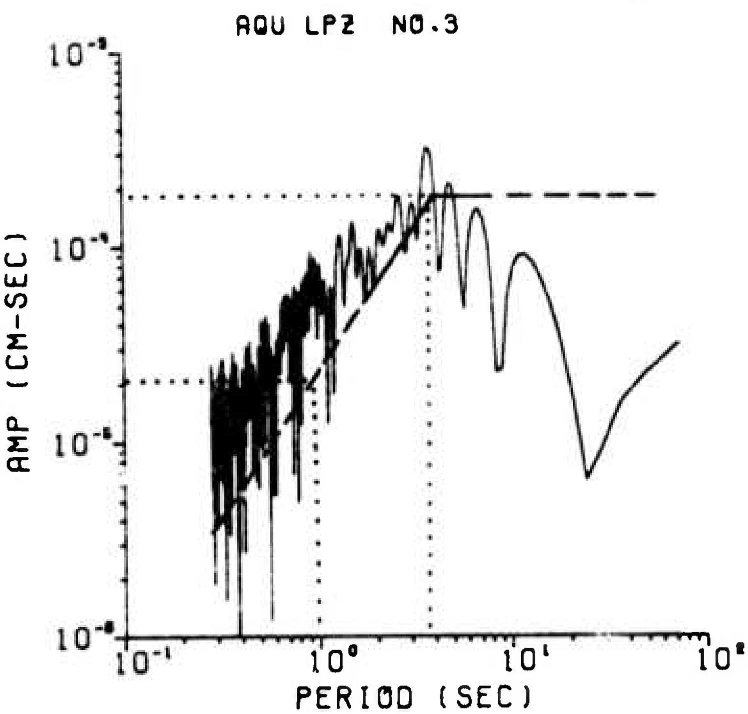

Figure 12c. Spectrum of vertical component of P-wave motion from long-period seismogram for earthquake 3 of 16 August 1971, as recorded at Aquila, Italy.

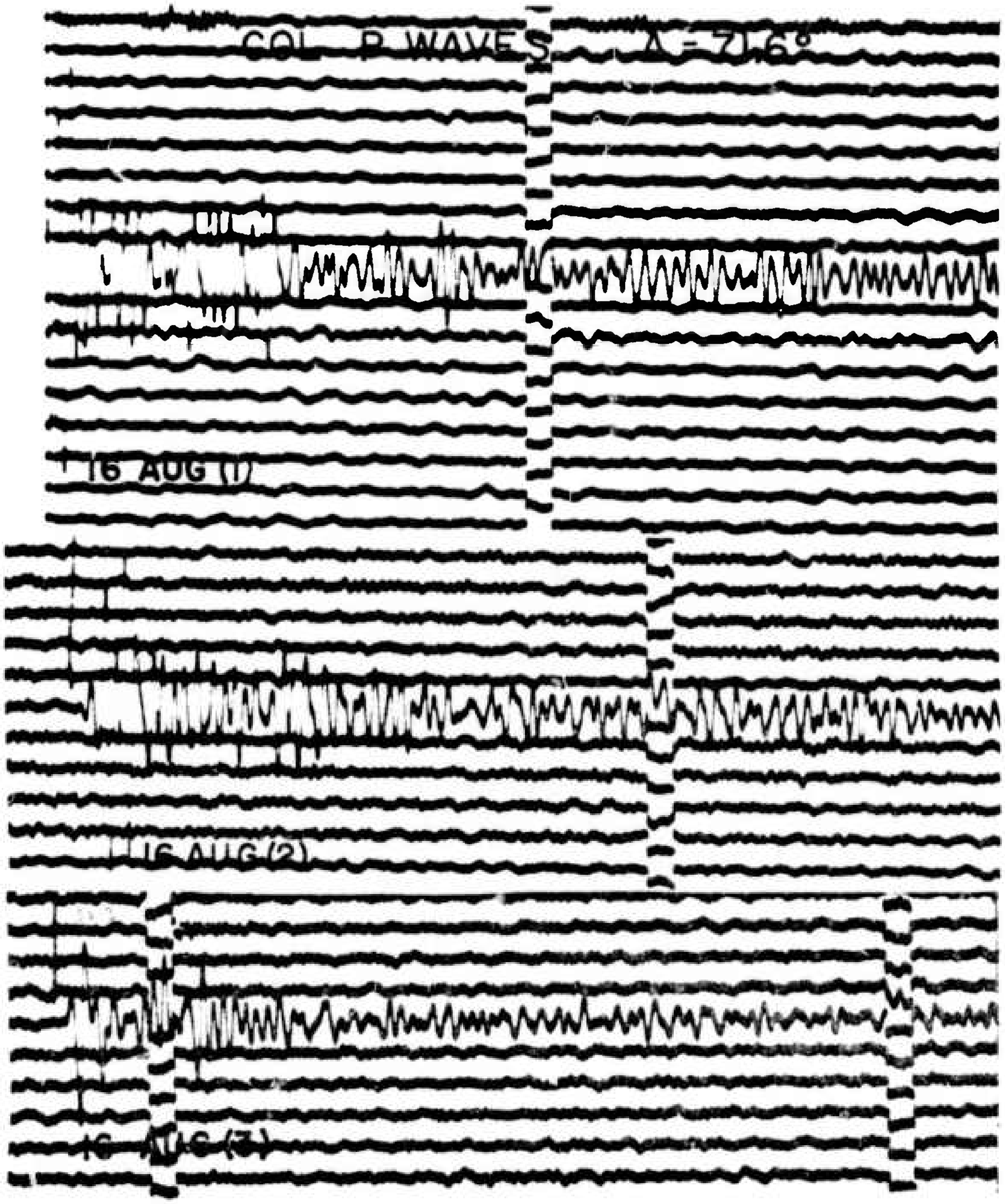

Figure 13. Vertical-component P waves for earthquakes of 16 August 1971 as recorded by short-period seismographs at College, Alaska.

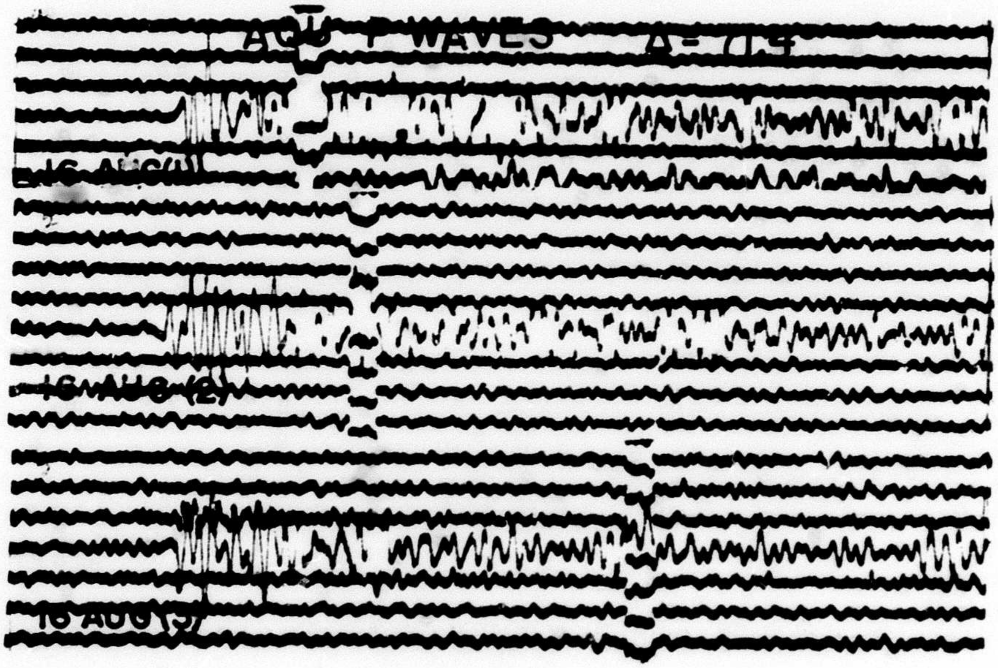

Figure 14. Vertical-component P waves for earthquakes of 16 August 1971 as recorded by short-period seismographs at Aquila, Italy.

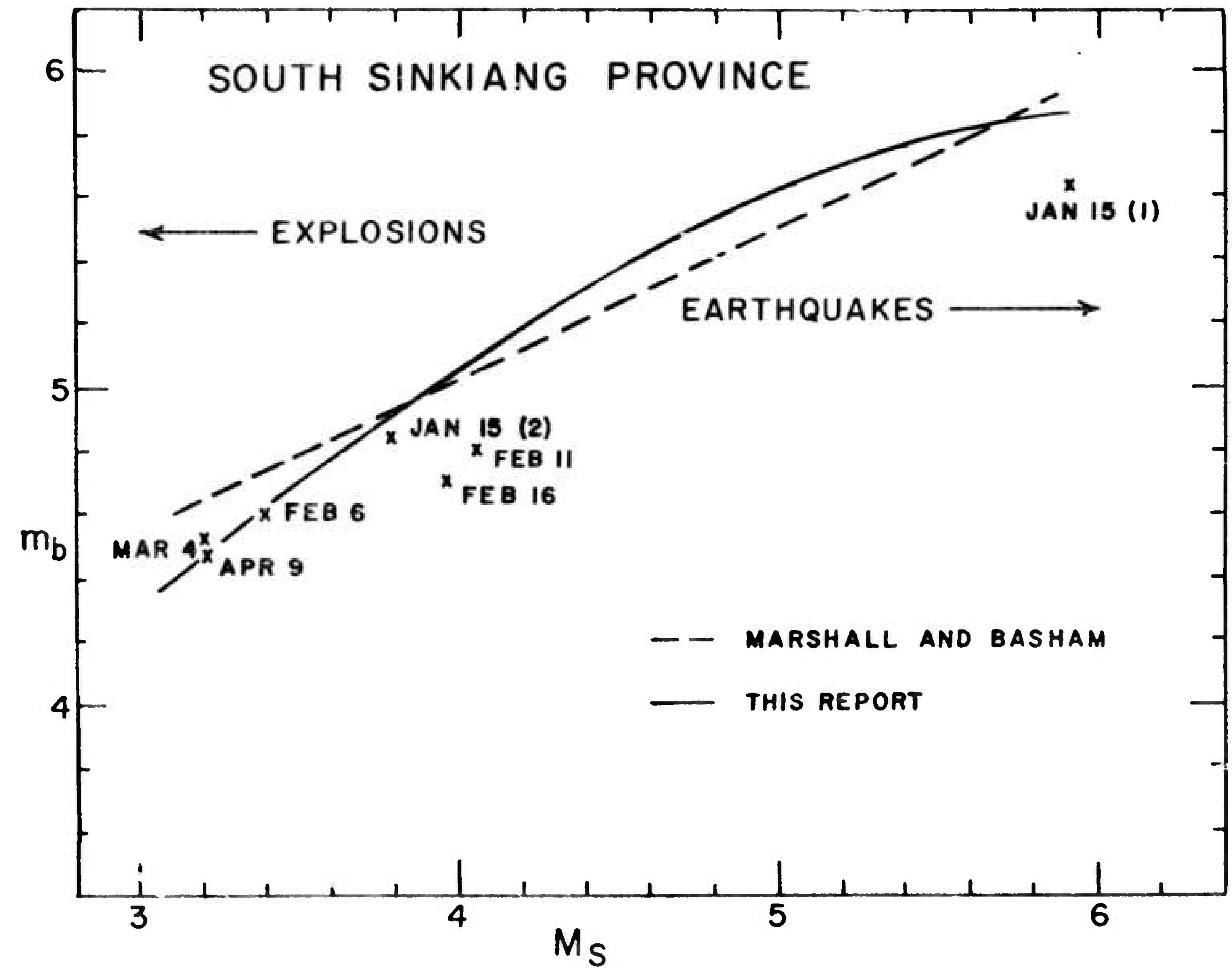

Figure 15. m_b vs M_S values for south Sinkiang, China aftershock sequence of January-April 1972.

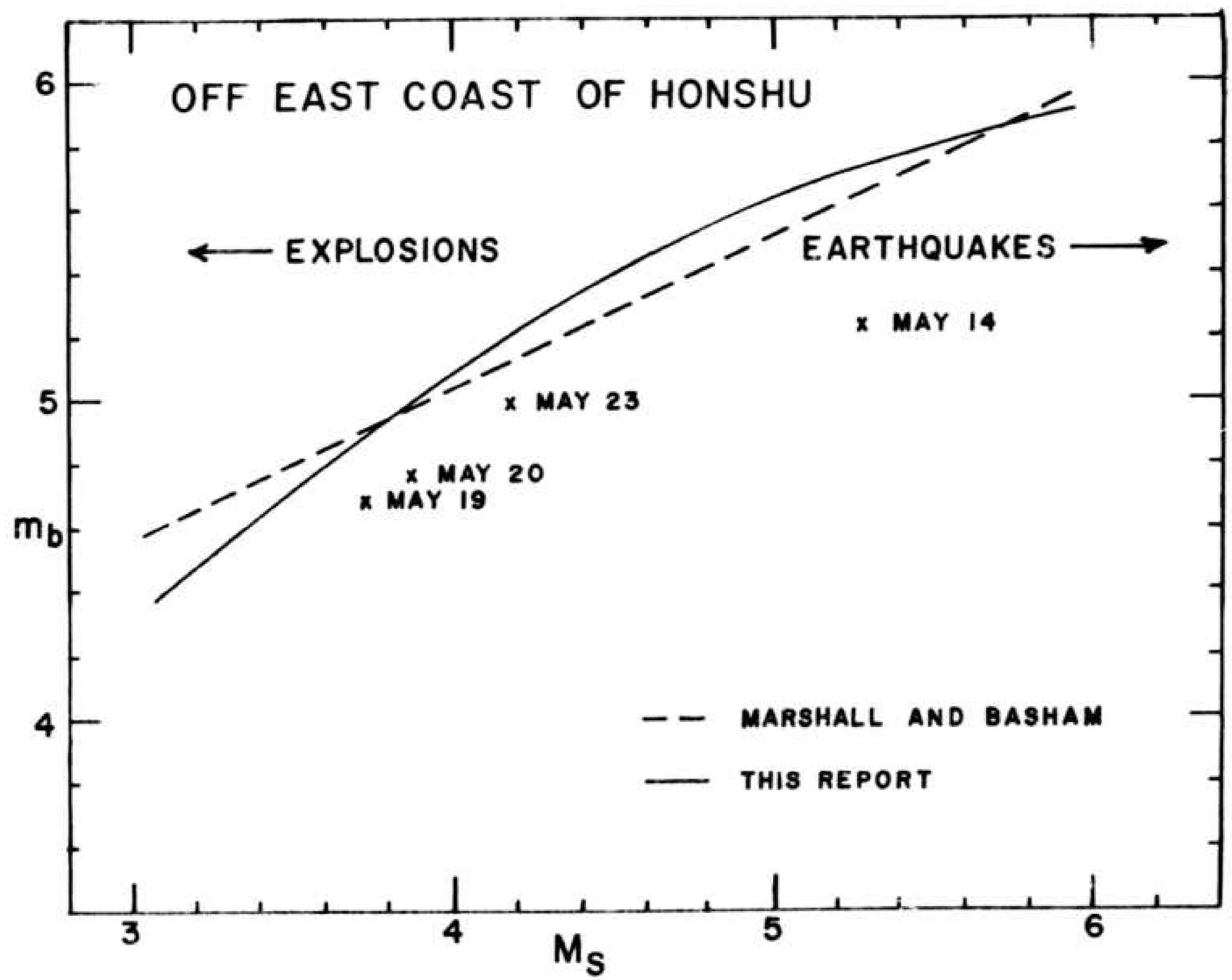

Figure 16. m_b vs M_S values for aftershock sequence of May 1972 off the east coast of Honshu Island.